Journal of Sedimentary Research

SEPM
1926
Society for
Sedimentary Geology

CORRELATIVE CONFORMITY OR SUBTLE UNCONFORMITY? THE DISTAL EXPRESSION OF A SEQUENCE BOUNDARY IN THE UPPER CRETACEOUS MANCOS SHALE, HENRY MOUNTAINS REGION, UTAH, U.S.A.

ZHIYANG LI* AND JUERGEN SCHIEBER
Department of Earth and Atmospheric Sciences, Indiana University, Bloomington, Indiana 47405, U.S.A.
e-mail: lizhiyanglee@gmail.com

ABSTRACT: In models of siliciclastic sequence stratigraphy, the sequence boundary in distal marine environments, where the strata are mudstone dominated, is usually considered a correlative conformity—the seaward extension of a subaerial unconformity. Despite its wide usage in the literature, objective recognition criteria of a correlative conformity remain lacking, largely due to the limited number of case studies directly examining the characteristics of sequence boundaries in offshore mudstone-dominated environments. This study focuses on the mudstone-dominated transitional interval between the Tununk Shale Member and the Ferron Sandstone Member of the Mancos Shale Formation exposed in south-central Utah to extend our understanding of the characteristics of a sequence boundary developed in the distal shelf environment of a ramp setting. An integrated sedimentologic, petrographic, and sequence stratigraphic analysis was conducted to characterize the sequence boundary that separates the Tununk from the Ferron depositional system (hereafter referred to as the T-F sequence boundary) and its lateral along-depositional-strike variability.

Although manifest as a mudstone-on-mudstone contact, the T-F sequence boundary in all three measured sections is a subtle unconformity, characterized by erosional truncation below and onlap above, and marks a distinct basinward shift in facies association. The T-F sequence boundary also marks the change from the Tununk offshore mud-belt system to the Ferron Notom delta system, and therefore represents a surface that divides two genetically different depositional systems. Based on two distinct marker beds that bracket the T-F sequence boundary, the T-F sequence boundary can be traced across the study area with confidence. The lateral variability in the characteristics of the T-F sequence boundary along depositional strike indicates that it was produced by an allogenic base-level fall.

Offshore shelfal mudstone strata may contain a significantly higher incidence of subtle unconformities analogous to the T-F sequence boundary than currently appreciated. Careful sedimentologic and petrographic analyses, combined with lateral correlations constrained by reliable chronostratigraphic marker beds, are essential for identifying subtle unconformities in shelf mudstone successions. The accurate recognition of subtle unconformities in mudstone strata is critical to apply the sequence stratigraphic approach appropriately to distal shelf environments, as well as to better constrain the timing and cause (allogenic vs. autogenic) of relative changes of sea level recorded in these rocks.

INTRODUCTION

Sequence stratigraphy provides a useful analytical approach to study rock relations in a time-stratigraphic framework based on changes in facies, the geometric character of strata, and identification of key bounding surfaces (Mitchum et al. 1977; Posamentier and Vail 1988; Van Wagoner et al. 1990). Although sequence stratigraphic models differ from each other, depositional sequences share the common definition that they are repetitive, genetically related strata separated by sequence boundaries which are surfaces of erosion or nondeposition, or their correlative conformities (Mitchum et al. 1977; Posamentier and Vail 1988; Van Wagoner et al. 1988; Neal et al. 2016; Catuneanu 2019). Clearly, the

correct identification of sequence boundaries is critical for the practice of sequence stratigraphy as a whole.

When sequence boundaries were first defined on the basis of seismic stratigraphy, their recognition criteria included onlap, downlap, toplap, and erosional truncations, which are indicators of nondepositional or erosional hiatuses (Mitchum et al. 1977). Sequence-bounding unconformities, which occur mainly at the basin margin, often lose seismic expression when traced basinward, and the term "correlative conformity" has been included as the distal equivalent of the unconformity that has "no physical evidence of erosion or nondeposition and no significant hiatus" (Mitchum et al. 1977). By this definition, a correlative conformity identified on seismic profiles in more basinal settings may still be an unconformity with which the associated subtle stratal termination—evidence of erosion or nondeposition—is below seismic resolution. Therefore, to determine whether a sequence boundary in distal marine environments is truly a correlative conformity or a subtle unconformity characterized by hiatus of

---

*Present Address: Department of Geology, Colorado College, Colorado Springs, Colorado 80903, U.S.A.

relatively short duration requires detailed sedimentologic analysis in outcrop or core (Mitchum et al. 1977; Miller et al. 2013).

Although the recognition criteria and chronostratigraphic significance of sequence boundaries have been extensively investigated in outcrops, cores, or geophysical well logs (Ainsworth and Pattison 1994; Miall and Arush 2001; Catuneanu et al. 2009; Bhattacharya 2011; Holbrook and Bhattacharya 2012; Li and Bhattacharya 2013; Korus and Fielding 2017; Pattison 2019), most prior studies have focused on sequence boundaries formed in coastal to shallow marine environments commonly comprising sandstone-dominated strata. Based on distinct erosional truncations (e.g., the base of incised-valley fills) or drastic facies change (e.g., the juxtaposition of nonmarine on marine facies), sequence boundaries formed in coastal and nearshore environments can be relatively readily recognized (Van Wagoner et al. 1990; Shanley and McCabe 1995; Bhattacharya 2011; Korus and Fielding 2017).

Objective recognition criteria of sequence boundaries in distal mudstone-dominated marine environments, based on detailed sedimentary facies characteristics, remain lacking. This is because detailed sedimentologic and stratigraphic analyses of fine-grained sedimentary rocks are usually more time-consuming due to their susceptibility to weathering, overall homogeneous appearance, and rather subtle variability in grain size and sedimentary features upon cursory inspection. Nevertheless, advances from flume studies and an increasing number of detailed sedimentologic and petrographic analyses of ancient mudstone-dominated successions have amply demonstrated that mudstones can be deposited under substantially more energetic and dynamic depositional conditions than previously presumed and contain a wealth of features indicative of erosional or nondepositional hiatuses (Bohacs and Schwalbach 1992; Bohacs 1998; Schieber 1998, 2016; Bohacs et al. 2002; Lazar 2007; Macquaker et al. 2007; Schieber et al. 2007; Aplin and Macquaker 2011; Plint 2014; Wilson and Schieber 2014; Li et al. 2015; Trabucho-Alexandre 2015; Birgenheier et al. 2017; Kemp et al. 2018; Li and Schieber 2020). A better understanding of the processes that govern the transport and deposition of fine-grained sediments makes it a timely endeavor to re-examine in detail how sequence boundaries are expressed in offshore mudstone-dominated successions. Are sequence boundaries in distal mud-dominated environments indeed conformities and thus (in practice) difficult or impossible to identify? The accurate recognition of sequence boundaries in distal mudstone-dominated successions is critical for the genetic subdivision of seemingly homogeneous offshore mudstone strata and their integration into sequence stratigraphic models. Being the most common sedimentary rock type, refining the sequence stratigraphic appraisal of mudstones will greatly enhance the utility of these rocks as important paleoenvironmental archives and add predictive power when these rocks are evaluated as unconventional hydrocarbon reservoirs.

This study focuses on the transitional interval between the Tunuk Shale Member and the overlying Ferron Sandstone Member of the Upper Cretaceous Mancos Shale to improve the characterization of sequence boundaries in distal shelf environments. Previous studies indicate that both the Tunuk Shale and Ferron Sandstone were deposited on a storm-dominated shelf (i.e., the Western Interior Seaway) in a ramp setting (Kauffman 1985; Ericksen and Slingerland 1990). Early sequence stratigraphic models emphasized a passive-margin setting (a shelf–slope setting; Mitchum et al. 1977; Posamentier and Vail 1988), whereas sequence stratigraphic models in a ramp setting have been discussed only briefly (Van Wagoner et al. 1990). Existing sequence stratigraphic models in a ramp setting (Van Wagoner et al. 1990; Posamentier et al. 1992; Neal et al. 2016; Catuneanu 2019) all suggest that a sequence boundary would change from erosional or nondepositional unconformity in proximal settings to its correlative conformity in distal offshore settings, where the strata are mudstone-dominated (e.g., below fair-weather wave base; Fig. 1). However, the conformable nature of a sequence boundary in distal shelf environments should not be assumed (Ayranci et al. 2018; LaGrange et al.

2020) without thorough examination because these models tend to highlight sand-dominated environments around fair-weather wave base and are usually conceptual or model-driven (Posamentier et al. 1992; Catuneanu 2019).

The main objectives of this study are to characterize the sedimentary facies of the mudstone-dominated transitional interval between the Tunuk Shale and the Ferron Sandstone in detail, and to develop a depositional and sequence stratigraphic framework within which the sedimentary character of the sequence boundary between the Tunuk and Ferron (the T-F sequence boundary) can be more closely examined. Detailed sequence stratigraphic frameworks of both members have been developed (Zhu et al. 2012; Li and Schieber 2020), providing useful constraints on the stratigraphic position of the sequence boundary separating the two genetically different depositional systems (hereafter referred to as the T-F sequence boundary). The exceptionally well-exposed transitional interval between the Tunuk Shale and the Ferron Sandstone offers an excellent opportunity to pinpoint the T-F sequence boundary, as well as to closely examine its sedimentary character and lateral variability along depositional strike.

This study indicates that the T-F sequence boundary is a subtle unconformity upon close inspection, although it would likely be characterized as a correlative conformity based on the original definition of sequence boundary. In all three measured sections, the T-F sequence boundary represents a hiatus that is locally characterized by truncation below and onlap above, even though in every instance it is characterized by a mudstone-on-mudstone contact. These observations suggest that offshore mudstone strata likely contain unconformities that are more subtle than previously considered.

GEOLOGICAL SETTING

The Tunuk Shale Member and the Ferron Sandstone Member of the Mancos Shale Formation accumulated along the western margin of the Late Cretaceous (middle to late Turonian) Western Interior Seaway (Fig. 2), which was situated in a broad foreland basin that had formed due to flexural loading by the Sevier thrust belt to the west (Kauffman 1985; Li and Aschoff 2022a). In response to sediments supplied from the Sevier orogenic belt to the west, Upper Cretaceous sedimentary strata along the western margin of the seaway show multiple eastward prograding sandy clastic wedges that grade basinward into thick marine mudstone successions. Deposits of the foreland basin record a series of transgressive–regressive successions that have been interpreted as being driven mainly by second-order eustatic sea-level cycles and partly by regional and local tectonic processes (Kauffman 1985; Miall et al. 2008; Li and Aschoff 2022b). One of these cycles is termed the Greenhorn cycle, which began in the late Albian and ended in the late Turonian (Fig. 3). In south-central Utah, early to middle Turonian strata of the Tunuk Shale Member were deposited across the maximum transgression and during the subsequent regression of the Greenhorn cycle (Fig. 3). The culmination of the regressive phase during the Greenhorn cycle is marked by deposition of the overlying Ferron Sandstone, which was deposited as a deltaic clastic wedge that is informally named the Notom delta in the study area (Peterson et al. 1980; Bhattacharya and Tye 2004) (Fig. 2).

During deposition of both the Tunuk Shale and the Ferron Sandstone, circulation in the Western Interior Seaway was dominated by storms, resulting in longshore currents and net sediment drift directed predominantly to the south along the western margin of the seaway (Ericksen and Slingerland 1990; Li et al. 2015). Previous studies based on detailed sedimentologic facies characteristics suggest that the Tunuk Shale was deposited as an offshore mud belt on a storm-dominated shelf (Li and Schieber 2018a) and the Ferron Sandstone as a storm-influenced to storm-dominated deltaic environment (Peterson et al. 1980; Bhattacharya and Tye 2004; Li et al. 2011; Zhu et al. 2012). Due to the progradation of the
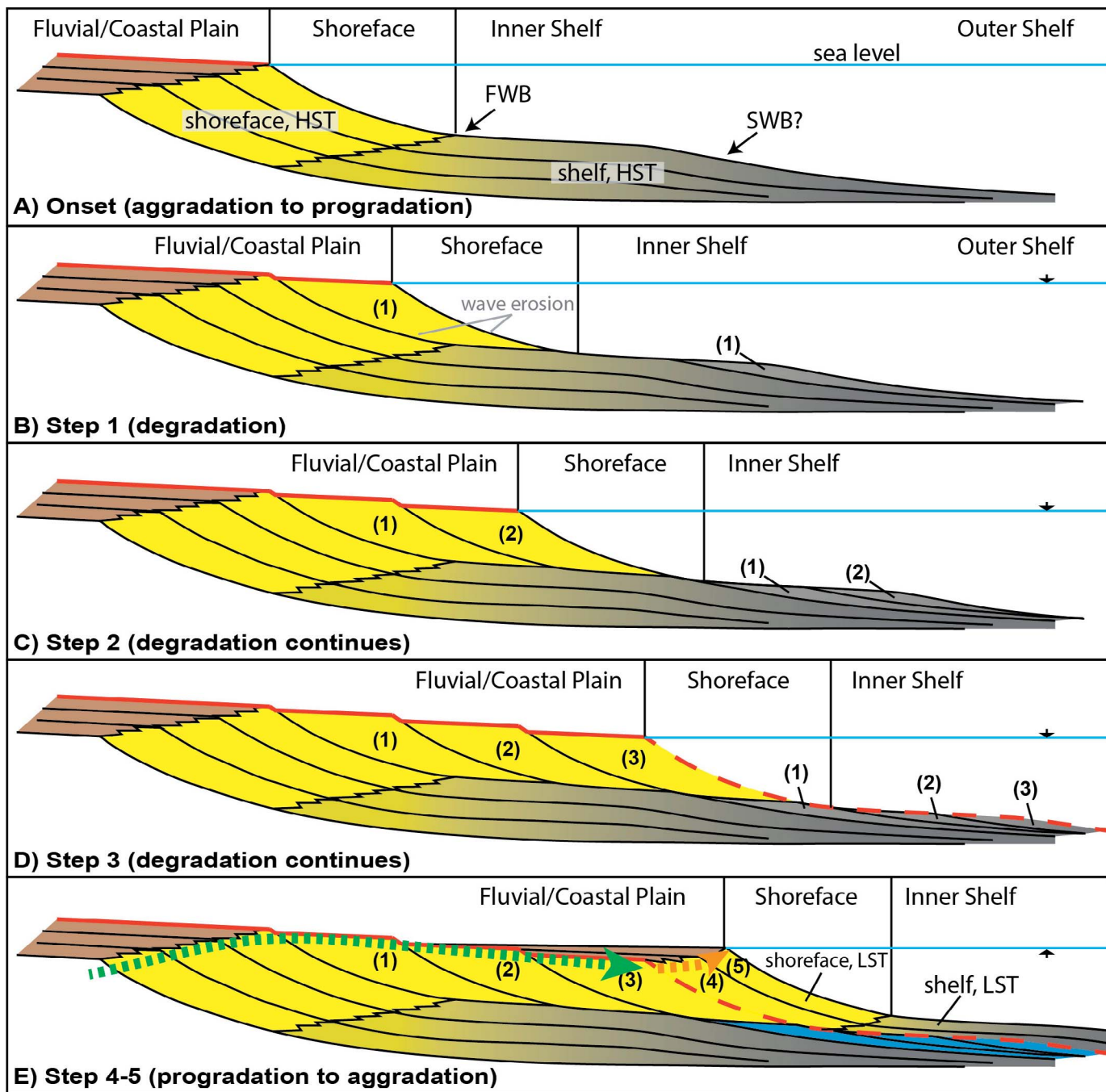
FIG. 1.—Schematic drawing illustrating the formation of a correlative conformity during sea-level fall in a shelf or ramp setting (modified from Posamentier et al. 1992; Catuneanu 2006; Neal et al. 2016). In a proximal setting the sequence boundary is characterized by subaerial erosion and coastal onlap, whereas in a more distal setting the sequence boundary is characterized by a correlative conformity. The sequence boundary (including the subaerial unconformity and correlative conformity) can be objectively picked based on coastal onlap (in the most proximal setting) and the change from APD to PA (Neal et al. 2016). The model shown here is very conceptual because: 1) the clinoform slope is vertically exaggerated and 2) the clinothem geometry is simplified and does not conform to many natural clinothem systems on modern continental shelves (Pirmez et al. 1998; Patruno et al. 2015).
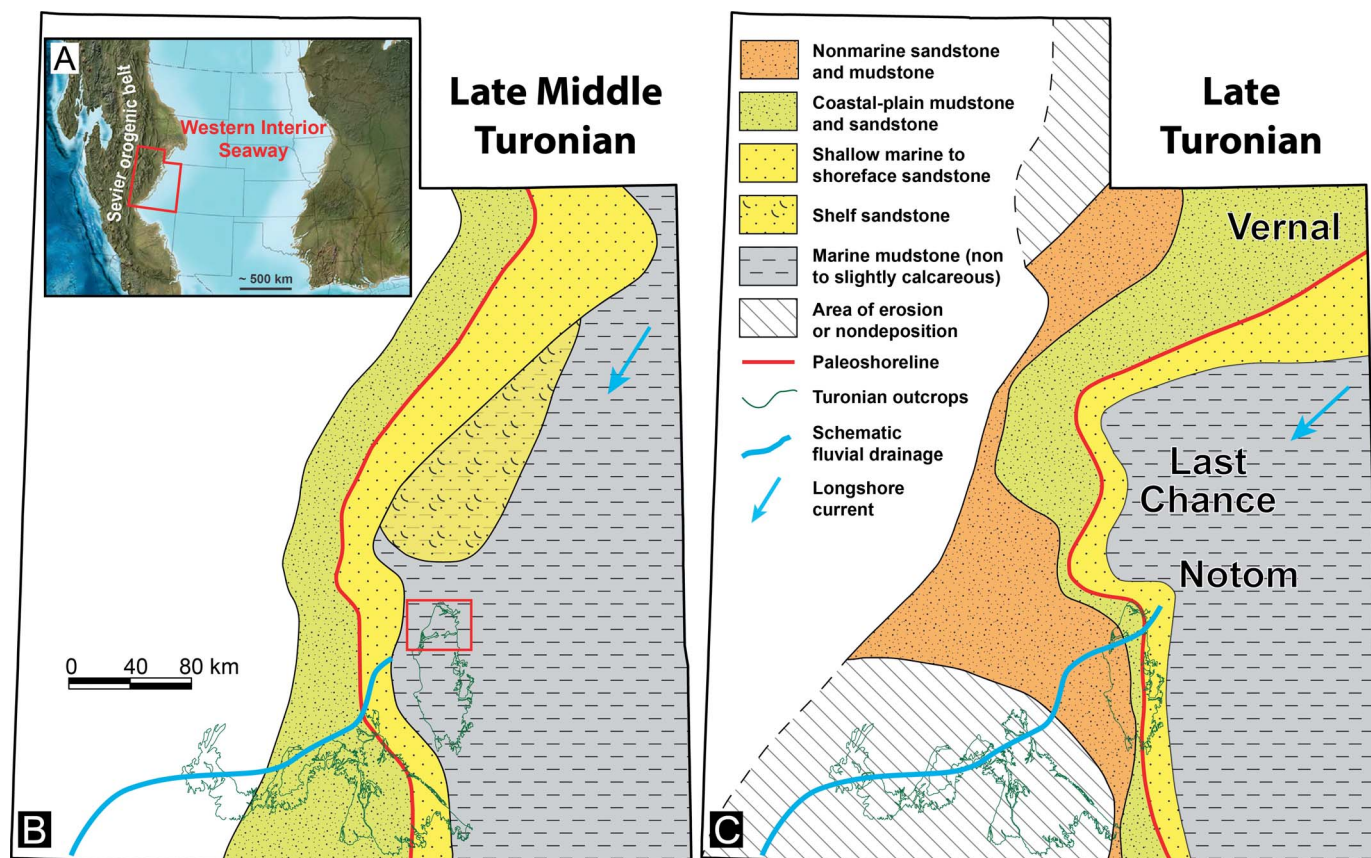
FIG. 2.—**A)** Middle Turonian paleogeographic map illustrating the extent of the Western Interior Seaway (Blakey 2014). Utah is highlighted in red. **B)** Late middle Turonian paleogeographic reconstruction of Utah during deposition of the upper part of the Tununk Shale Member. The red box indicates the study area in the northern Henry Mountains region. **C)** Late Turonian paleogeographic reconstruction of Utah during deposition of the Ferron Sandstone Member. The Ferron Sandstone consists of three deltaic clastic wedges that were informally named the Vernal (northeastern Utah), Last Chance (central Utah), and Notom (in our study area) delta systems. Paleogeographic maps are reconstructed based on multiple sources (Elder and Kirkland 1994; Gardner 1995; Primm et al. 2018; Li and Schieber 2018a). The transitional interval studied here was deposited between the times represented by Parts B and C.

Notom delta system, the paleoshoreline in our study area gradually evolved from trending northeast–southwest during the deposition of the Tununk Shale to northwest–southeast during deposition of the Ferron Sandstone (Fig. 2).

METHODS AND STUDY AREA

This study focuses on the well-exposed transitional interval between the Tununk Shale and the Ferron Sandstone located in the northern part of the Henry Mountains region, west of Hanksville, Utah (Fig. 4). Examination of the transitional interval during outcrop reconnaissance indicates that the T-F sequence boundary that marks the onset of the Ferron Notom delta system is constrained stratigraphically by a set of three bentonite (altered volcanic ash) marker beds (hereafter referred to as the bentonite triplet) below and an interval of fine mudstones rich in fossil (inoceramid and ammonoid) fragments and phosphatic particles (hereafter referred to as the condensed mudstone interval) above. Both the bentonite triplet and the condensed mudstone interval are laterally continuous and traceable across our study area, providing excellent chronostratigraphic constraints for the T-F sequence boundary. Detailed sedimentologic sections that span the interval from the lowest bentonite bed to a few meters above the condensed mudstone interval were measured bed-by-bed at three localities (Salt Wash, Steamboat, and North Caineville; Fig. 4).

For each measured section, sedimentological data including lithology, grain size, sedimentary structures, bioturbation features (trace fossil types,

bioturbation intensity), the relative abundance and general types of fossil fragments, and the relative abundance of land-plant debris were documented. The Bioturbation Index (BI) of (Taylor and Goldring 1993) was used to characterize the bioturbation intensity in the studied interval. In the field, grain size variability was mainly determined by: 1) feeling and chewing rock samples to estimate silt versus clay content (i.e., gritty versus smooth) and 2) color variations. Because the studied interval consists dominantly of mudstones, the naming scheme proposed by (Lazar et al. 2015) was adopted here to further classify different types of mudstones based on their composition and grain size—a coarse mudstone has more than two-thirds of coarse mud (32 to 62.5 μm) grains, a fine mudstone has more than two-thirds of fine mud ($<$ 8 μm) grains, whereas a medium mudstone has neither coarse nor fine mud in excess of two-thirds of the mud-size grains.

More than 50 fairly fresh (without apparent weathering) rock samples were collected from outcrops throughout each measured section. All collected samples were then embedded in epoxy, slabbed, and polished (with up to 800 grit sandpaper) in the laboratory. High-resolution images of polished slabs were acquired with a flatbed scanner (up to 2400 dpi resolution) and then contrast-enhanced in Adobe Photoshop to reveal millimeter- to centimeter-scale variations in sedimentary characteristics. Descriptive terms for the thickness, continuity, shape, and geometry of lamina and bed from (Campbell 1967) were adopted here. Sedimentary and biogenic features described in the field and on polished slabs were
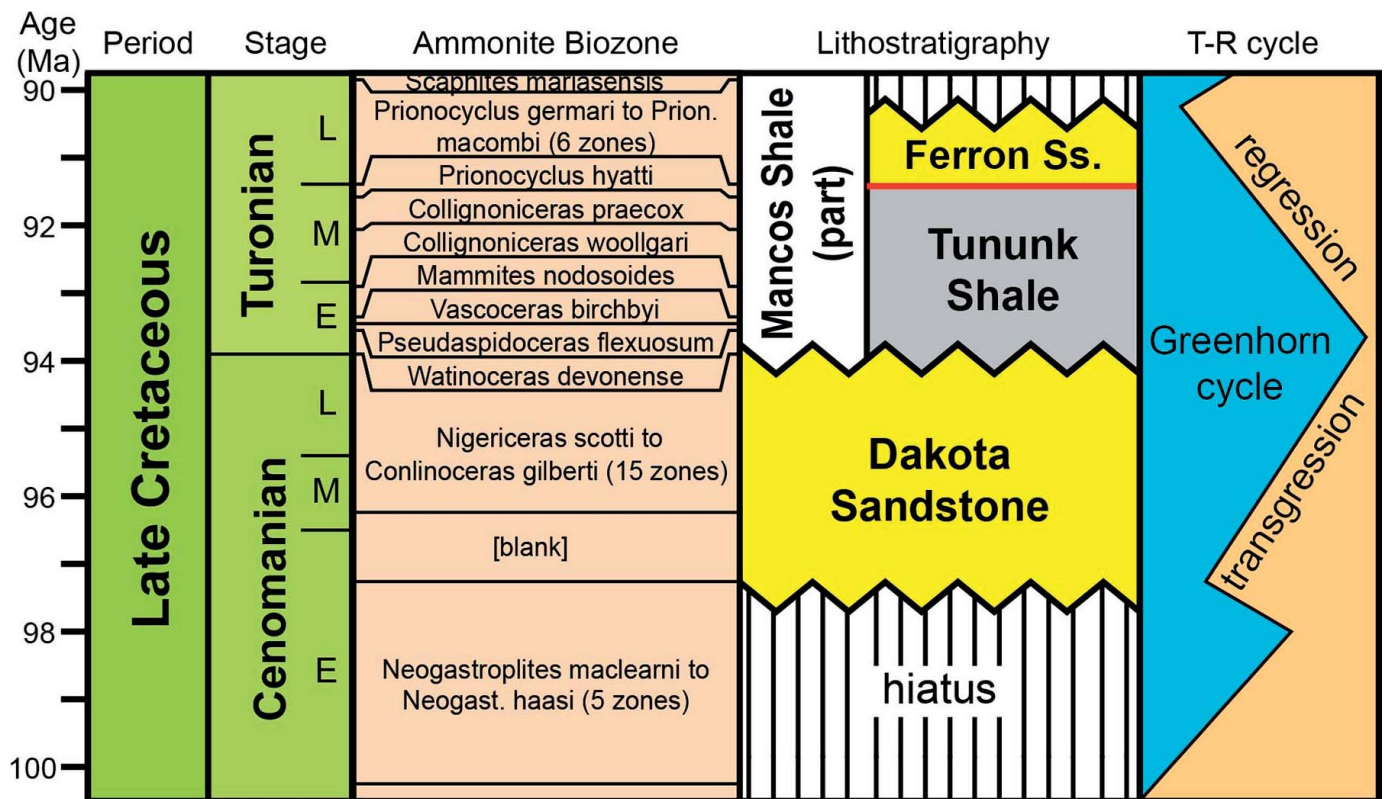
FIG. 3.—Cenomanian to Turonian stratigraphy in the Henry Mountains region, south-central Utah (Zelt 1985; Leithold 1994; Leithold and Dean 1998). Absolute dates are from Ogg et al. (2012). T-R cycle is from Kauffman (1985). The thick red line between the Tununk Shale and Ferron Sandstone members approximately indicates the temporal extent of the studied interval. It is important to point out that the boundary between two lithostratigraphic units (e.g., Tununk Shale Member and Ferron Sandstone Member) is almost always arbitrarily defined. This study particularly focuses on the sequence boundary separating the genetic Tununk from Ferron depositional systems rather than the arbitrary lithostratigraphic boundary.

combined to comprehensively characterize facies variations, infer depositional processes and conditions, and aid in sequence stratigraphic interpretations. For sequence stratigraphic analysis, this study focused on the most fundamental and objective characteristics of parasequences, system tracts, and sequences. Parasequences are characterized by distinctive upward-shallowing successions of relatively conformable beds and bedsets bounded by surfaces of flooding, abandonment, or reactivation and their correlative surfaces (Van Wagoner et al. 1990; Catuneanu et al. 2009; Neal et al. 2016). Based on parasequence stacking patterns, position in the sequence, and types of bounding surfaces, different system tracts can be identified (Van Wagoner et al. 1990); specifically lowstand, transgressive, and highstand system tracts (LST, TST, and HST; Vail 1987; Van Wagoner et al. 1988). Key stratal surfaces that divide sequences into different system tracts include the sequence boundary (SB), the transgressive surface (TS), and the maximum-flooding surface (MFS; Van Wagoner et al. 1990).

Five polished thin sections (20 to 25 μm thick), made from representative samples of distinctly different facies associations, were examined by both optical and scanning electron microscopes. Additional ion-milled samples for SEM analysis were made from samples close to (< 1 m above and below) the T-F sequence boundary at Salt Wash and Steamboat. Information derived from petrographic observations provided additional insights into the interpretation of depositional processes and the sequence stratigraphic framework. Variations in the petrographic composition and provenance of rock samples throughout the studied interval, particularly across the T-F sequence boundary, were examined. Based on combined sedimentologic and petrographic analysis, variations in the facies characteristics across the T-F sequence boundary and lateral facies variations of the T-F sequence boundary can be comprehensively characterized.

DESCRIPTION AND INTERPRETATION OF FACIES ASSOCIATIONS

The transitional interval between the Tununk Shale and the Ferron Sandstone in the study area comprises four distinct facies associations (Fig. 5). All facies associations are composed dominantly of mudstone and varying amounts of sandstone. Detailed characteristics of all facies associations identified in this study are summarized in Table 1. The studied interval also contains common discrete bentonite beds and carbonate concretionary layers (Fig. 5), which were not included in any facies association and will not be discussed in this section. This is because the generation and deposition of volcanic ashes (i.e., volcanic eruptions) do not depend on any specific depositional environment, and carbonate concretions are early diagenetic products formed during periods of very slow sedimentation or breaks in sedimentation, when microbially driven diagenetic reactions allowed accumulation of calcite cements in pore spaces of surficial sediments (Raiswell 1988; Raiswell and Fisher 2000; Aplin and Macquaker 2011). In the context of this paper, the occurrence of bentonite beds or carbonate concretions does not yield any direct insights into the depositional environments of different facies associations. Nevertheless, the occurrence of bentonite beds and carbonate concretions have important implications for recognizing breaks in sedimentation and associated sequence stratigraphic surfaces (Lazar et al. 2015), which will be discussed in more detail below.
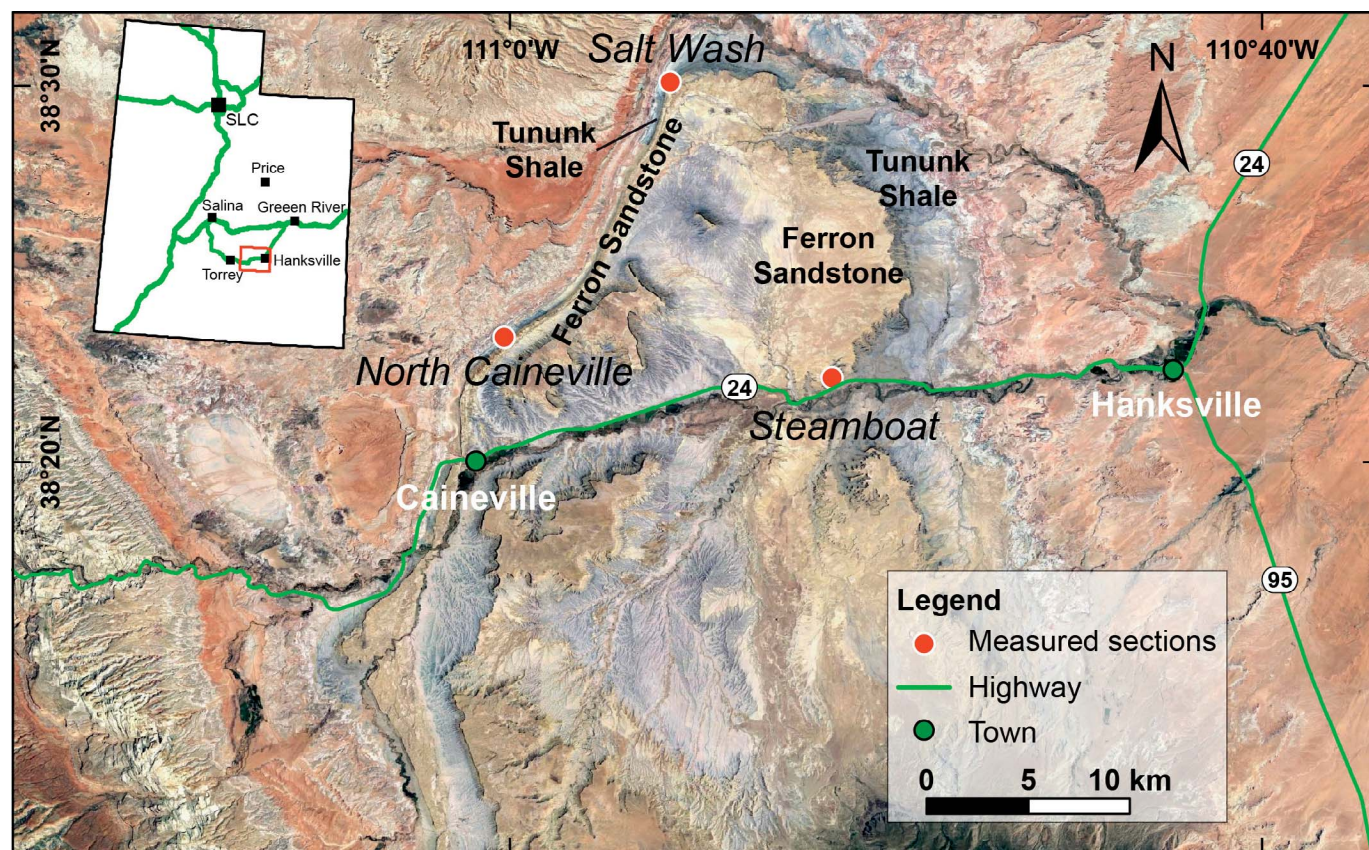
Fig. 4.—Map showing outcrop belts of the Tununk Shale and Ferron Sandstone near Hanksville. Red dots indicate the locations of three detailed sedimentologic sections measured in this study (Steamboat, Salt Wash, and North Caineville).

Facies Association 1

Facies association 1 (FA1) consists dominantly of gray, bioturbated, medium mudstone, commonly associated with laterally discontinuous coarse mudstone or sandstone laminae and beds (Figs. 5, 6). The BI of FA1 ranges from moderate (3–4) to high (BI 5–6), although some thin slightly bioturbated (BI 1–2) intervals are also present (Fig. 6C). Common types of trace fossils in FA1 include *Chondrites*, *Planolites*, *Phycosiphon*, *Teichichnus*, and occasional *Thalassinoides* (Fig. 6). Despite common bioturbation throughout FA1, many silty to sandy laminae and beds in FA1 can be recognized as disrupted, remnant wave-ripple lamination based on their overall symmetrical ripple crest (Fig. 6A–C). Although low-BI intervals are not very common in FA1, the decrease in BI of these intervals are usually accompanied by increases in the abundance, thickness, and lateral continuity of coarse mudstone and sandstone beds showing wave-ripple and combined-flow-ripple lamination (Fig. 6B–D). Dominant particles in FA1 are of siliciclastic origin, including quartz, feldspar, and clay minerals (Fig. 6E, F). Other minor components of FA1 include small amounts (< 5% in abundance) of fossil fragments (e.g., fish debris, inoceramid and ammonoid fragments) and land-plant debris. FA1 occurs at the basal part of all three measured sections (i.e., the uppermost part of the Tununk Shale; Fig. 5).

Facies Association 2

FA2 consists dominantly of dark gray, slightly bioturbated, fine and medium mudstones (Fig. 7). The BI of FA2 ranges from 1 to 2, and trace fossils in FA2 consists mostly of *Chondrites*, *Planolites*, and *Phycosiphon* (Fig. 7). Both the BI and trace-fossil diversity in FA2 are distinctly lower than FA1. Compared to FA1, FA2 is more distinctly laminated to thinly bedded (3–10 cm), consisting of common coarse mudstone or sandstone laminae and beds which are also more laterally continuous (Fig. 7). Coarse mudstone and sandstone layers in FA2 commonly show wave-ripple and some combined-flow-ripple lamination and small hummocky cross stratification (Fig. 7A–D). FA2 has the overall same petrographic composition as FA1, consisting mainly of siliciclastic particles and small amounts of fossil fragments and land-plant debris (Fig. 7E–F). FA2 is present only in the Salt Wash and North Caineville sections, lying directly above FA1 (Fig. 5).

Facies Association 3

FA3 consists dominantly of light gray, slightly bioturbated, medium and coarse mudstones with more common very fine sandstone. The BI of FA3 is overall very low (0–2), and intervals devoid of bioturbation are more common and thicker in FA3 (Fig. 8A, B). Trace-fossil diversity is even more limited in FA3, including mostly small *Chondrites*. FA3 is distinctly laminated to medium-bedded (10–30 cm). Sedimentary structures in FA3 include abundant grading (common normal grading and less frequent inverse grading; Fig. 8A, B), starved to current ripple cross lamination (Fig. 8A, B), massive bedding, parallel lamination/bedding, and soft-sediment deformation (e.g., ball-and-pillow structures and convolute bedding; Fig. 8C). FA3 contains a distinctly greater amount of coarse silt-size particles compared to FA1 and FA2. In addition to common siliciclastic particles, FA3 contains distinctly greater proportions of terrigenous organic matter (> 5% by volume). Fragments of land-plant debris are commonly found on bedding planes (Fig. 8D). Another component unique to FA3 is silt-size carbonate grains (dolomite and
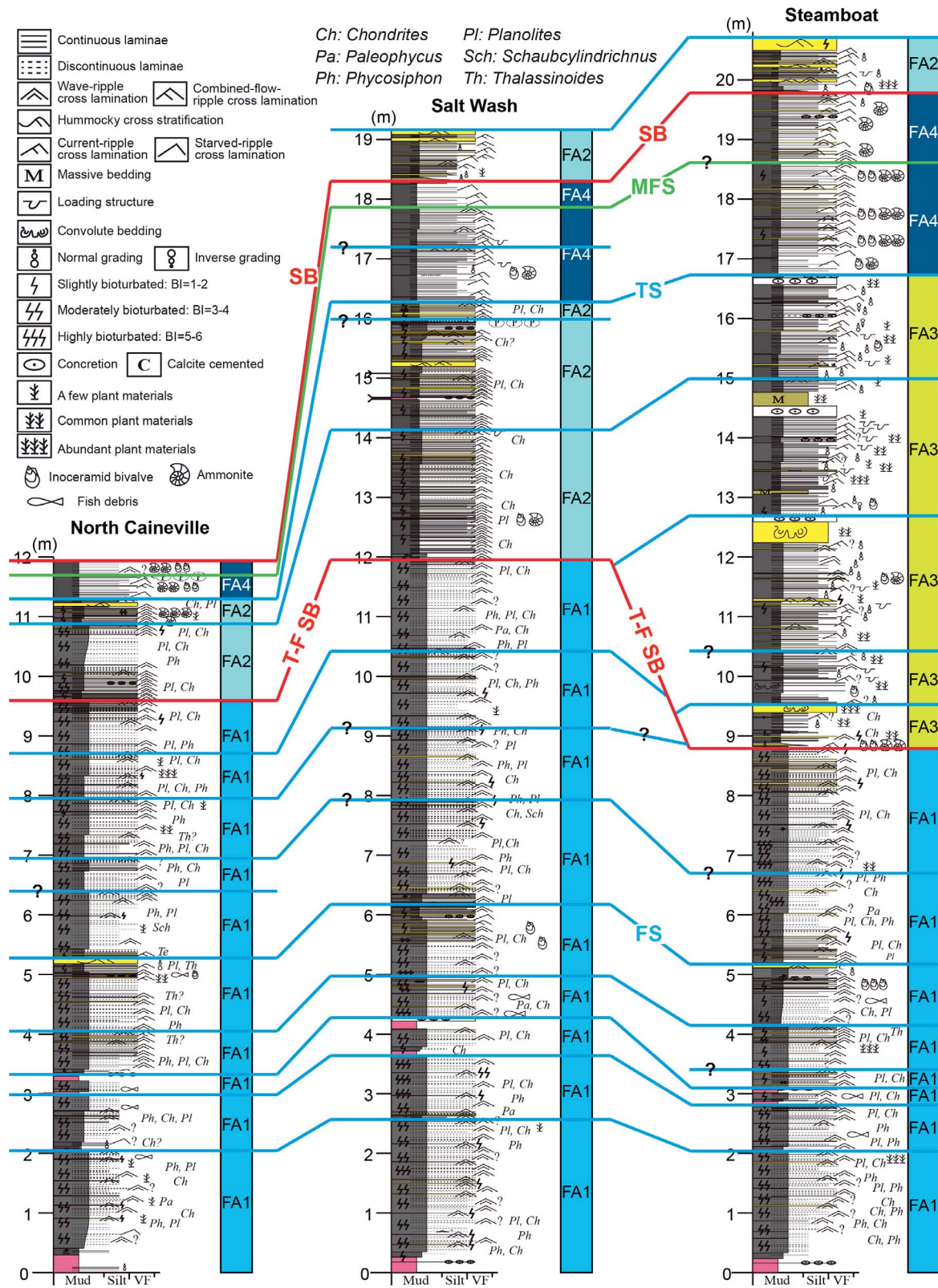
FIG. 5.—Detailed sedimentologic sections of the transitional interval between the Tununk Shale and Ferron Sandstone measured in this study, with types of facies associations present in each section. The correlation of three sections is based on sequence stratigraphic surfaces (i.e., FS, flooding surface; SB, sequence boundary; TS, transgressive surface; MFS, maximum flooding surface).

TABLE 1.—Summary of facies associations in the transitional interval between the Tununk Shale and the Ferron Sandstone.

Facies Associations (FA)	Petrographic Composition	Grain Size, Lamina/Bed Style	Sedimentary Structures/Features	Bioturbation Characteristics
FA1 (medial inner shelf)	Dominant siliciclastic mineral grains such as quartz, feldspar, and clay minerals; small amounts (< 5% in abundance) of fossil fragments (e.g., fish debris, inoceramid and ammonoid fragments) and land-plant debris	Gray, bioturbated, medium mudstone commonly associated with laterally discontinuous coarse mudstone or sandstone laminae and beds	Common disrupted, remnant wave-ripple lamination	BI 3–6, low BI (1–2) presents locally. Types of trace fossils: *Chondrites*, *Planolites*, *Phycosiphon*, *Teichichnus*, and occasional *Thalassinoides*
FA2 (proximal inner shelf)	Overall same petrographic composition as FA1, consisting mainly of siliciclastic particles and a small amounts of fossil fragments and land-plant debris	Dark gray, slightly bioturbated, fine and medium mudstones with common coarse mudstone or sandstone laminae and beds that are also more laterally continuous; distinctly laminated to thinly bedded (3–10 cm)	Wave-ripple and some combined-flow-ripple lamination and small hummocky cross stratification	BI 1–2. Types of trace fossils: *Chondrites*, *Planolites*, and *Phycosiphon*
FA3 (river-dominated prodelta)	Common siliciclastic particles and a distinctly greater proportion of land-plant debris (> 5% by volume); another unique component in FA3 is silt-size carbonate grains (dolomite and calcite)	Light gray, slightly bioturbated, medium and coarse mudstones with more common sandstone; distinctly laminated to medium-bedded (10–30 cm)	Abundant grading (common normal grading and less frequent inverse grading), starved to current-ripple cross lamination, massive bedding, parallel lamination/bedding, and soft-sediment deformation	BI 0–2. More common intervals devoid of bioturbation. Low trace fossil diversity, mostly small *Chondrites*
FA4 (distal inner shelf)	Siliciclastic particles and a much greater amount (> 10%) of fossil fragments (inoceramid, ammonoid, and fish debris) and phosphatic particles	Black, slightly bioturbated, fine mudstones with thin parallel coarse mudstone or sandstone laminae	Starved- to laterally continuous current-ripple cross lamination, wave ripple lamination, and gutter casts	BI 0–2. Low trace-fossil diversity

calcite; Fig. 8E, F). Although FA1 and FA2 contain some calcite fossil fragments, dolomite grains are absent in FA1 and FA2. FA3 is present only in the Steamboat section, occurring directly above FA1 (Fig. 5).

Facies Association 4

FA4 consists dominantly of black, slightly bioturbated, fine mudstones (Fig. 9). Among all four facies associations, FA4 contains the smallest amount of silt- and sand-size particles, and is the finest-grained facies association in the studied interval. The BI of FA4 is overall very low (BI 0–2), as is the trace-fossil diversity (Fig. 9). Common sedimentary structures present in FA4 include thin parallel coarse mudstone or sandstone laminae, starved to laterally continuous current-ripple cross lamination, wave-ripple lamination, and gutter casts (Fig. 9). The petrographic composition of FA4 significantly differs from the other three facies associations in that FA4 contains a much greater amount (> 10% and locally concentrated in millimeter- to centimeter-scale lag layers) of fossil fragments (inoceramid, ammonoid, and fish debris) and phosphatic particles (Fig. 9D). FA4 occurs in all three sections and occurs at the uppermost part of the studied interval (equivalent to the fine condensed mudstone interval), overlying FA2 at Salt Wash and North Caineville and FA3 at Steamboat (Fig. 5).

Interpretation of Depositional Environments

All facies associations (FA1 to FA4) are interpreted as deposited below fair-weather wave base because they are composed dominantly of mudstones and show trace fossils produced by deposit-feeding organisms. FA1, FA2, and FA4 are interpreted as deposited in a storm-dominated inner-shelf environment above storm wave base (up to ∼ 40 m water depth and ∼ 50 km offshore; Li and Schieber 2018a), based on the dominance of storm-generated sedimentary structures (i.e., wave-ripple and combined-

flow ripple lamination and minor hummocky cross stratification). An environment more distal than inner shelf for FA1, FA2, and FA4 is unlikely because biogenic calcareous particles (e.g., planktonic foraminifera tests, fecal pellets, and coccolith debris) that are common to abundant in middle- to outer-shelf deposits (*sensu* Li and Schieber 2018a) of the Tununk Shale are absent in these facies associations.

FA2 is interpreted as deposited in the shallowest, most proximal shelf environment (i.e., proximal inner shelf) among FA1, FA2, and FA4. The common, laterally continuous wave-ripple cross laminae, as well as overall low BI and trace-fossil diversity of FA2, indicate frequent storm events and a relatively high sedimentation rate (MacEachern et al. 2005). FA1 is interpreted as deposited in the medial inner-shelf environment, slightly more distal and in deeper water compared to FA2. Less common distinct storm-generated event beds and overall high BI of FA1 indicate decreased frequency and magnitude of storm events capable of influencing the seabed, providing longer post-event colonization windows (Bhattacharya et al. 2020). Bioturbation also commonly tends to disrupt or completely homogenize primary sedimentary structures, resulting in common remnant and disrupted laminations (likely wave-ripple) in medium mudstones (due to the mixing of silt or sand particles with fine mud particles by benthos; Fig. 6E) of FA1. FA4 is the finest-grained facies association and contains the least abundant wave-ripple laminae, suggesting deposition in the distal inner-shelf environment. The highest content of fossil fragments in FA4 also suggests a minimal degree of terrigenous clastic dilution. Nevertheless, FA4 still contains thin beds/laminae that exhibit storm-generated sedimentary structures, such as wave-ripple cross lamination and gutter casts (Fig. 8), indicating that its deposition was subject to storm-induced bottom currents.

FA3 is distinctly different from FA1, FA2, and FA4 and is interpreted as deposited in a river-dominated prodelta environment. It contains abundant
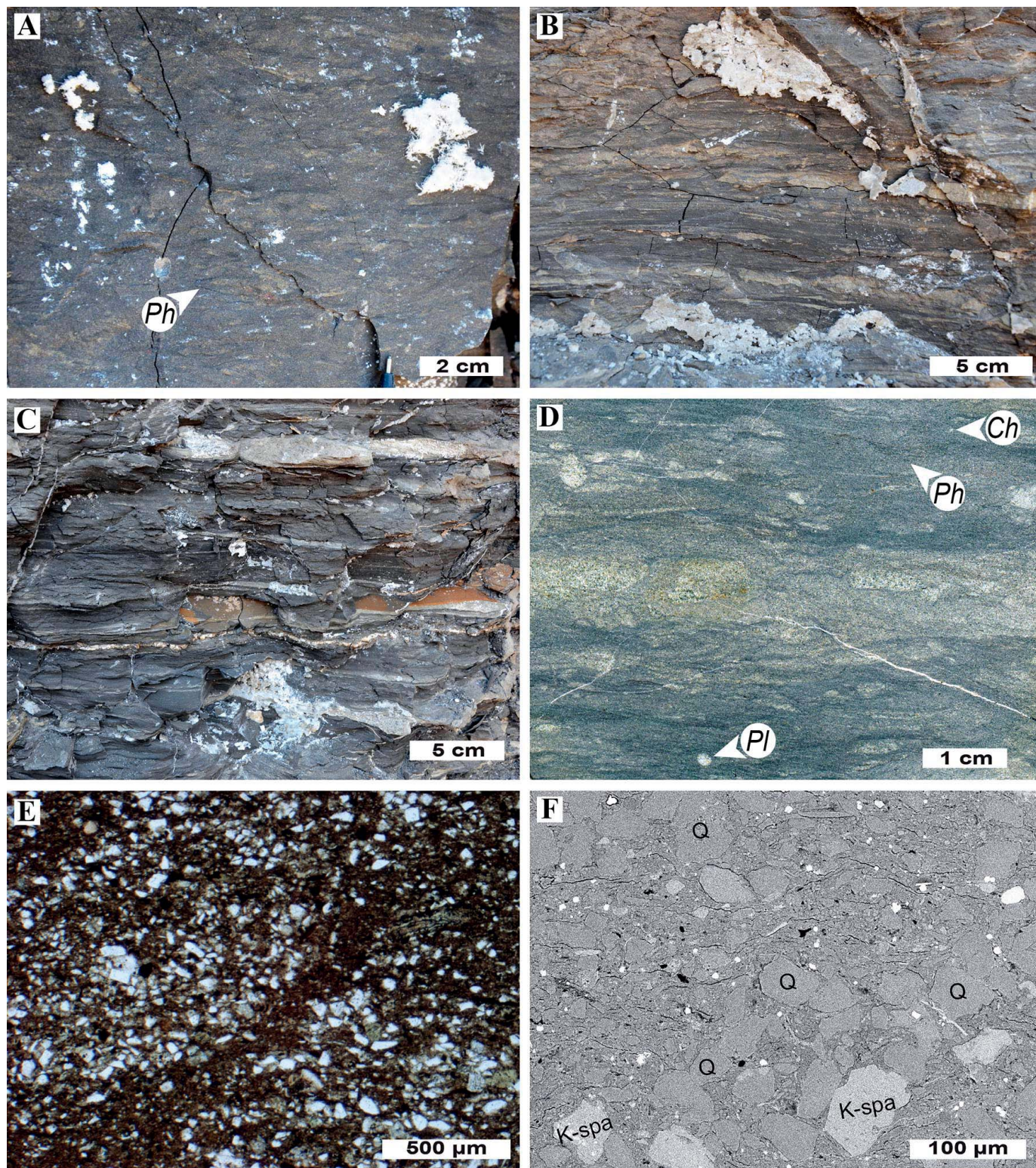
Fig. 6.—Sedimentologic and petrographic facies characteristics of FA1. **A**, **B)** Outcrop photos of moderately to highly bioturbated medium mudstones interbedded with a varying amount of remnant or disrupted silty or sandy wave-ripple laminae. **C)** Outcrop photo of slightly to moderately bioturbated fine to medium mudstones interbedded with some silty or sandy wave-ripple and combined-flow-ripple cross laminae. **D)** Scanned and processed images of polished slab showing moderately to highly bioturbated medium mudstones. The relatively coarse-grained middle area was probably a wave ripple originally and then disrupted by bioturbation. **E)** Photomicrograph (plane-polarized light) showing the commonly bioturbated texture in FA1. Note mixture of coarse mud and fine mud particles due to bioturbation. **F)** SEM photomicrograph (backscatter mode) showing that FA1 is composed mainly of siliciclastic minerals such as quartz, feldspar, and clay minerals. Q, quartz; K-spar, potassium feldspar.
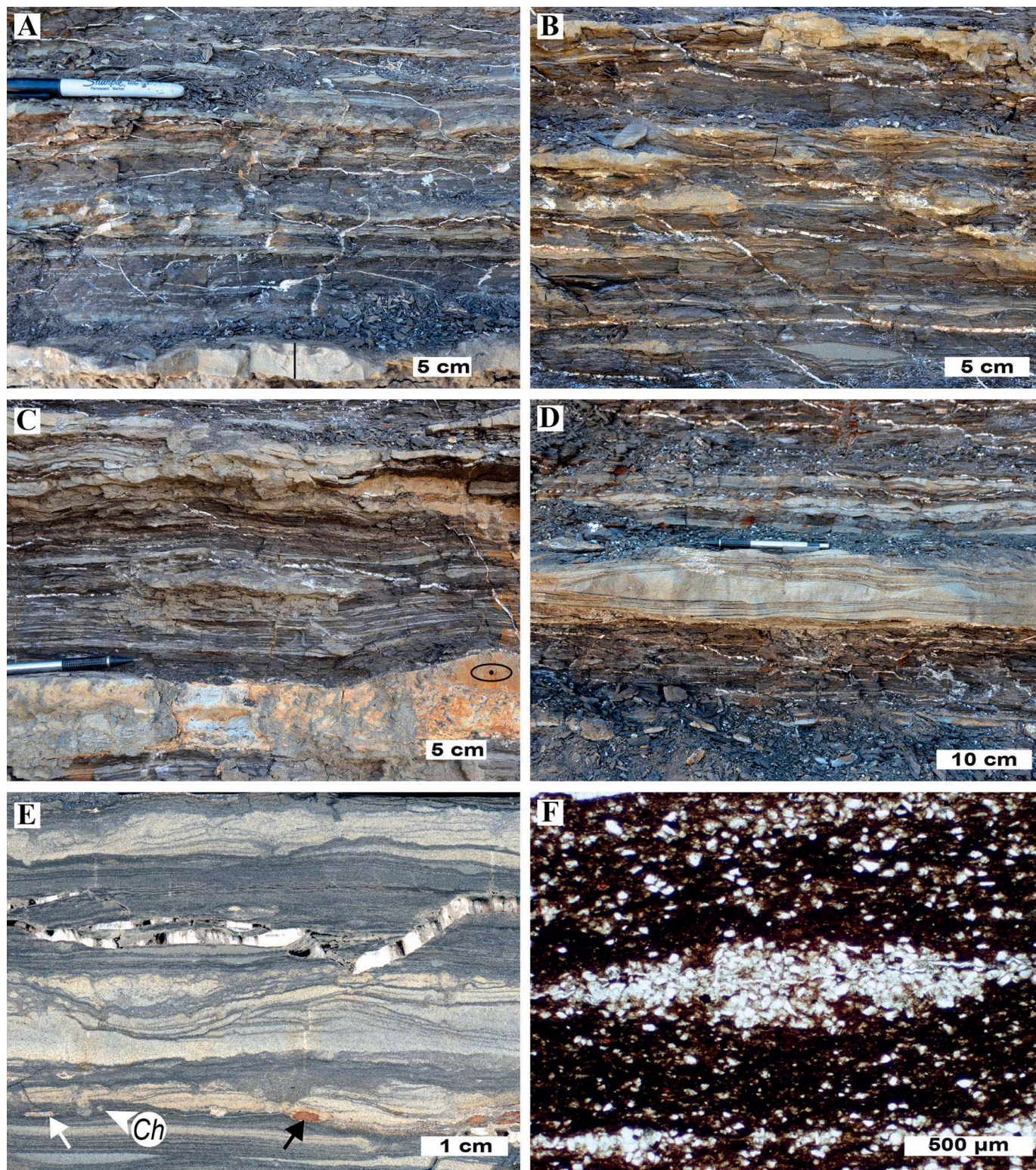
FIG. 7.—Sedimentologic and petrographic facies characteristics of FA2. **A–C)** Outcrop photos showing fine to medium mudstones interbedded with wave-rippled and combined-flow-rippled coarse mudstones to very fine sandstones. FBI is overall low. **D)** Outcrop photo of an ~ 10 cm thick sandstone bed showing hummocky cross stratification. **E)** Scanned and processed images of a polished slab showing slightly to moderately bioturbated FA2. Note common wave-ripple laminae. Ch, *Chondrites*. The white and black arrows indicate inoceramid debris and a phosphatic particle, respectively. **F)** Photomicrograph (plane-polarized light) showing well interlaminated fine mudstones and wave-rippled coarse mudstones.
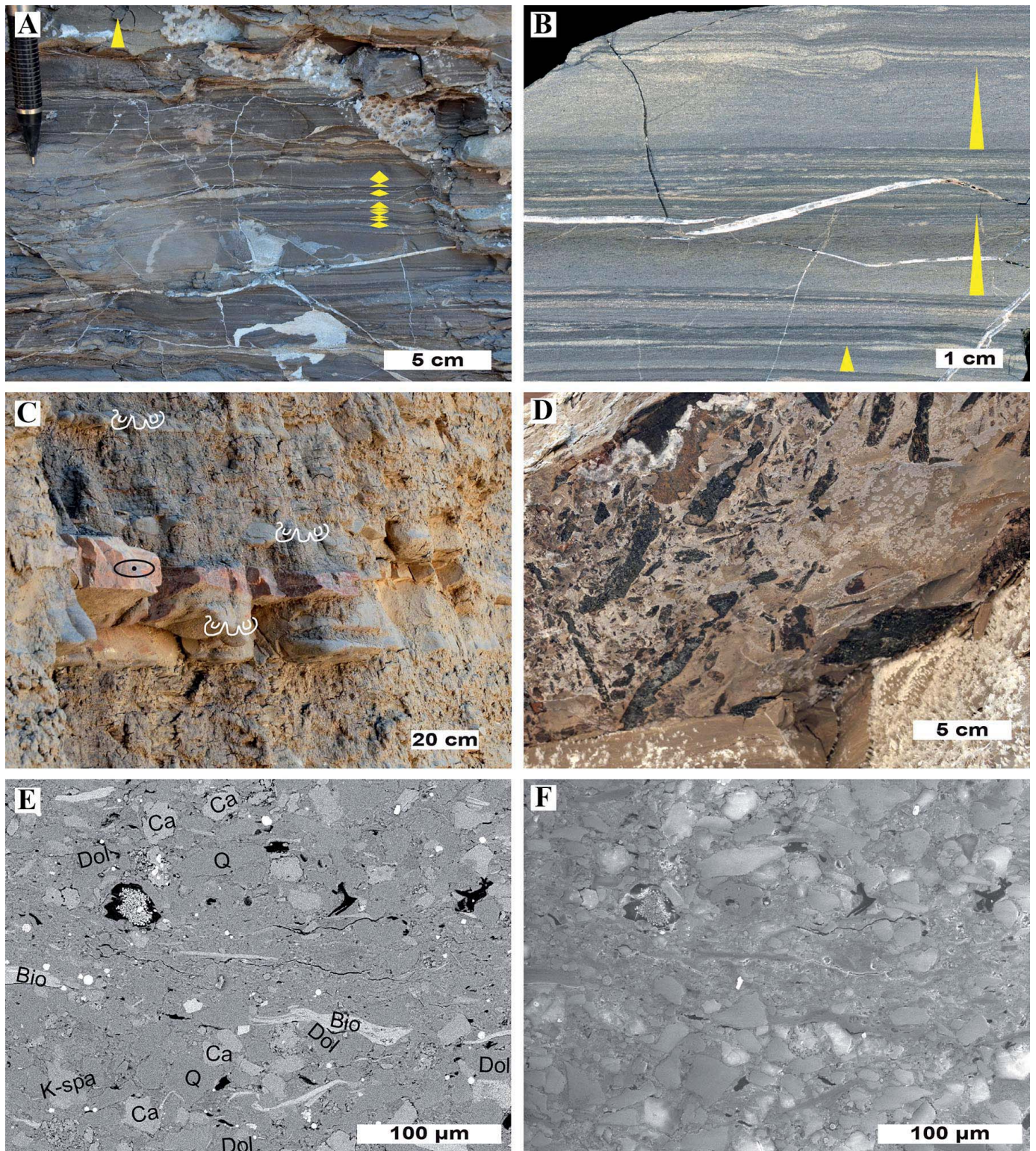
Fig. 8.—Sedimentologic and petrographic facies characteristics of FA3. **A)** Outcrop photo of coarse mudstones showing common grading (normal and inverse grading are indicated by yellow triangles) and asymmetrical-ripple cross lamination. **B)** Scanned and processed images of a polished slab of coarse mudstones showing normal grading and asymmetrical-ripple cross lamination. **C)** Outcrop photo of an FA3-dominated interval containing common ball-and-pillow structures (soft-sediment deformation). Refer to Figure 5 for symbols of sedimentary structures. **D)** Outcrop photo of a bedding plane showing abundant land-plant debris. **E, F)** SEM photomicrographs (backscatter and secondary electron mode) of the same area showing the petrographic composition of FA3. In addition to common siliciclastic particles (quartz, feldspar, and biotite), FA3 contains common silt-size carbonate particles (calcite and dolomite), which are interpreted to be of detrital origin. Carbonate particles can be distinguished from siliciclastic particles based on the much brighter color in the secondary electron image (Part F) due to the charging effect. Calcite and dolomite can then be distinguished from each other based on their different backscatter coefficients (Part E). Energy-dispersive X-ray spectroscopy (EDS) was also used to aid determination of mineralogy. Q, quartz; K-spar, potassium feldspar; Bio, biotite; Ca, calcite; Dol, dolomite.
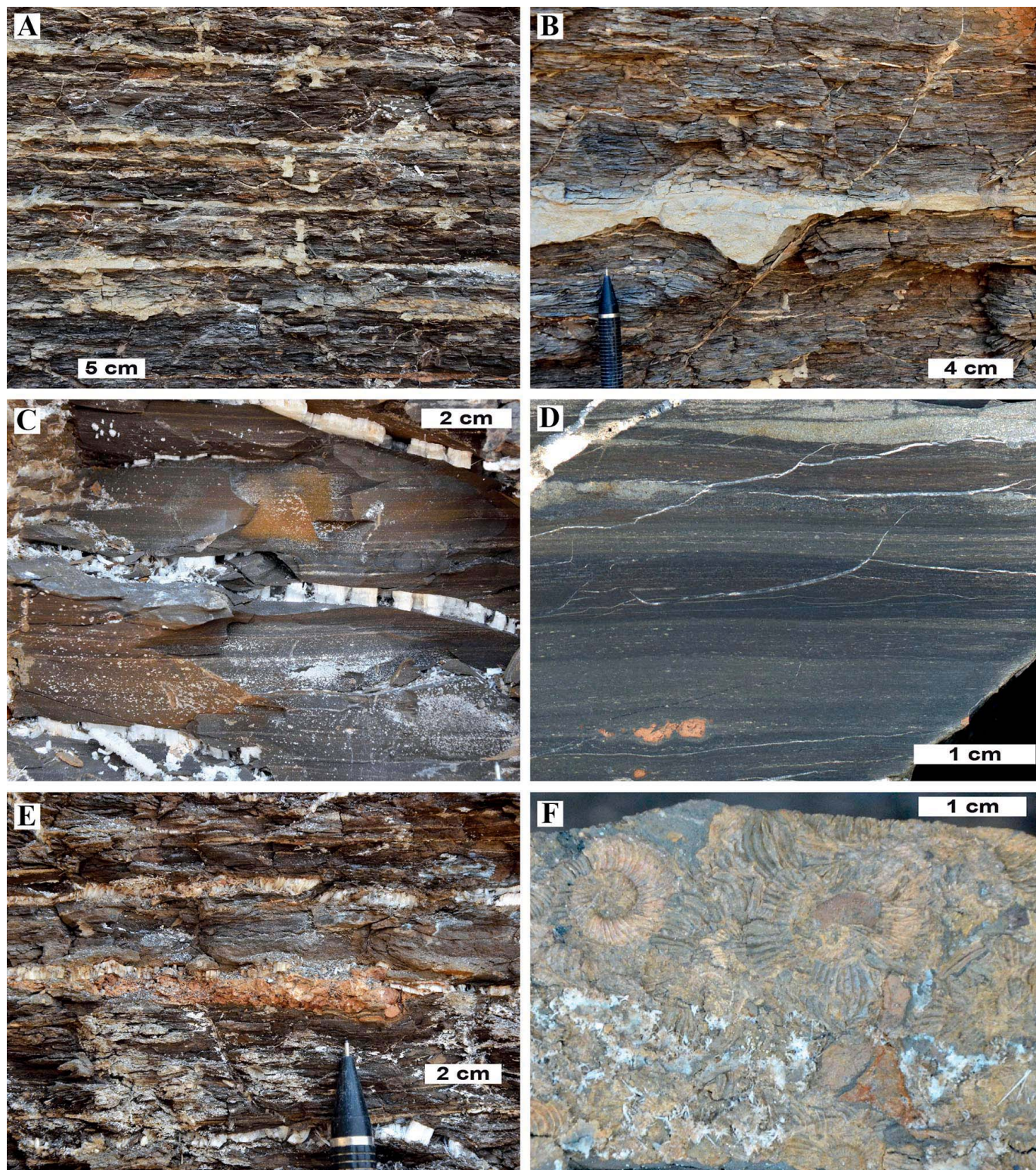
FIG. 9.—Sedimentologic facies characteristics of FA4. **A)** Outcrop photo of fine mudstones with thin coarse mudstone beds commonly showing symmetrical-wave-ripple lamination. **B)** Outcrop photo of a coarse mudstone bed showing a gutter cast. **C)** Outcrop photo of fine mudstones with common coarse mudstone laminae. **D)** Scanned and processed images of a polished slab of a fine-mudstone sample which contains common wavy laminae and wave-ripple lamination (upper right corner). Note the presence of common phosphatic particles (white arrows) and fossil fragments (white specks). **E)** Outcrop photo of a thin lag layer made mostly of phosphatic particles (above the pencil tip) in fine mudstones. **F)** A bedding plane in FA4 showing abundant ammonoid fragments.
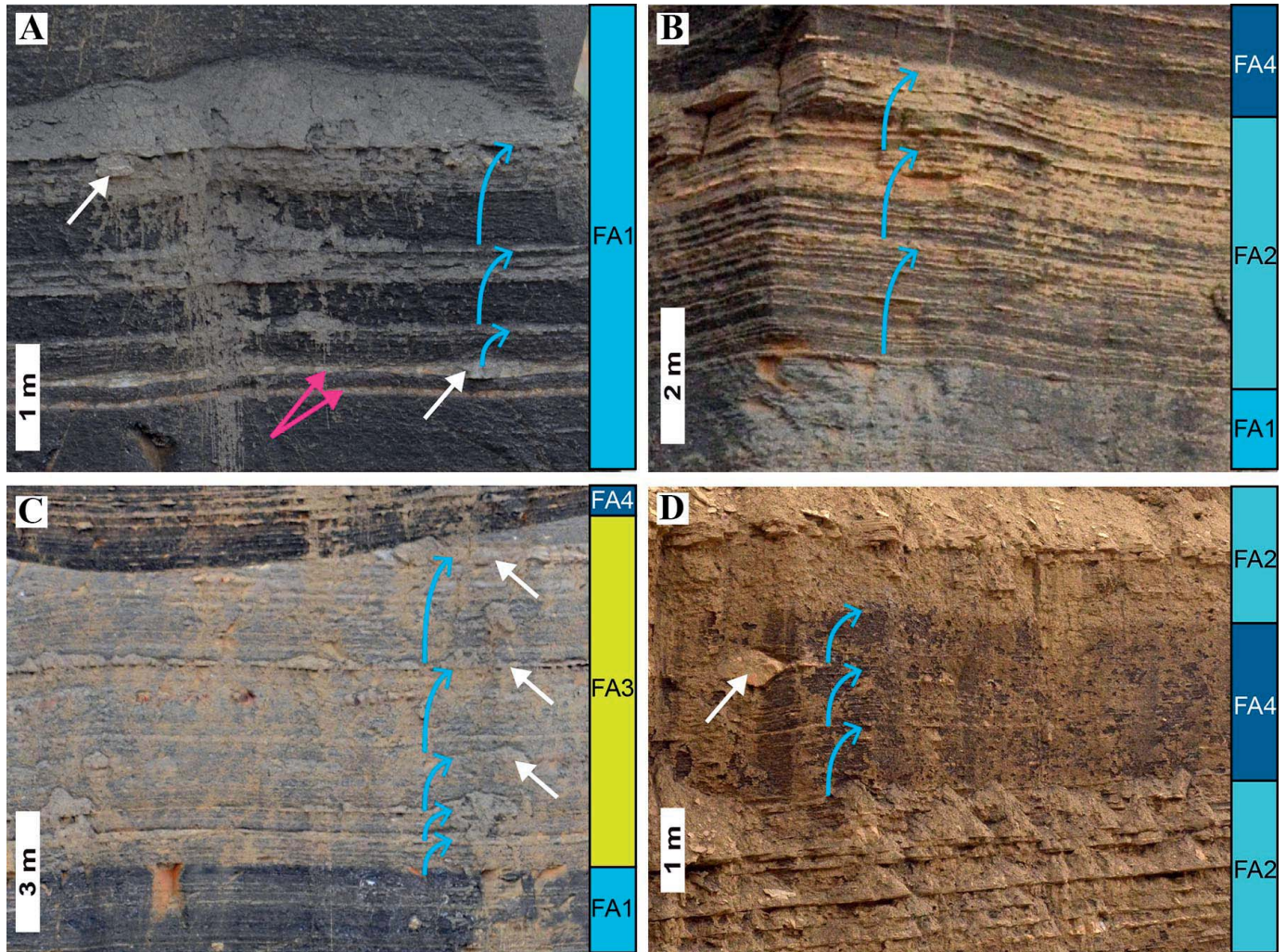
FIG. 10.—Parasequence styles in **A)** FA1, **B)** FA2, **C)** FA3, and **D)** FA4. Parts A and C are from Steamboat. Parts B and D are from Salt Wash. The coarsening-upward trend of parasequences is indicated by blue arrows. White arrows mark carbonate concretionary layers. Pink arrows in Part A mark the uppermost two bentonite beds of the bentonite triplet. See Figure 5 for detailed measured sections.

current-ripple cross lamination, indicative of the dominant influence of unidirectional flows. Common normal and inverse grading in FA3 can plausibly be attributed to waning surge-type turbidity currents and waxing-and-waning hyperpycnal flows, currents commonly generated in a river-dominated prodelta environment (Bhattacharya and MacEachern 2009; Li et al. 2015). The overall low BI, extremely low trace-fossil diversity, and common presence of soft-sediment deformation and fragments of land-plant debris in FA3 indicate very rapid sedimentation likely associated with the high sediment supply from a river.

SEQUENCE STRATIGRAPHIC FRAMEWORK OF THE TRANSITIONAL INTERVAL BETWEEN THE TUNUNK SHALE AND THE FERRON SANDSTONE

Parasequence Styles

Parasequences recognized in all four facies associations show an overall coarsening-upward trend via upward increases in siliciclastic silt and sand content (Figs. 5, 10). In the medial inner-shelf environment, FA1 parasequences do not always exhibit a distinct upward increase in average grain size due to common to complete bioturbation, which strongly disrupts silty or sandy event layers and mixes coarse mud to sand particles with fine mud particles (Fig. 6C). Nevertheless, the recognition of

parasequences in FA1 is aided by changes in bioturbation characteristics and sedimentary features. Generally, the bottom part of a parasequence is characterized by relatively low BI (as low as 1–2), thin (a few to several millimeters) starved-ripple, and occasional wave-ripple lamination (Fig. 5). Upward in a given parasequence, BI tends to increase (> 3–4), as does the abundance of disrupted, remnant silty or sandy wave-ripple laminae (Fig. 10A). Upward increases in the abundance of wave-ripple laminae, although commonly disrupted, in a given FA1 parasequence reflects a slight increase in sedimentation rate related to shallowing water depth. The higher BI in the upper part of some FA1 parasequence indicates that shallower water depth in the medial inner-shelf environment plays a more significant role in forming favorable substrate conditions (e.g., increases in food and oxygen supplies) than imposing more environmental stress due to higher sedimentation rate as proposed by Heath (1977) for modern sediments and Bohacs et al. (2005) for ancient strata.

The coarsening-upward trend of FA2 parasequences is readily apparent in outcrop (Fig. 10B). This is probably due to the overall low BI in the proximal inner-shelf environment. The thickness, lateral continuity, and abundance of silty to sandy laminae and beds that show storm-generated sedimentary structures usually increase upward distinctly in a given parasequence in FA2 (Fig. 10B).
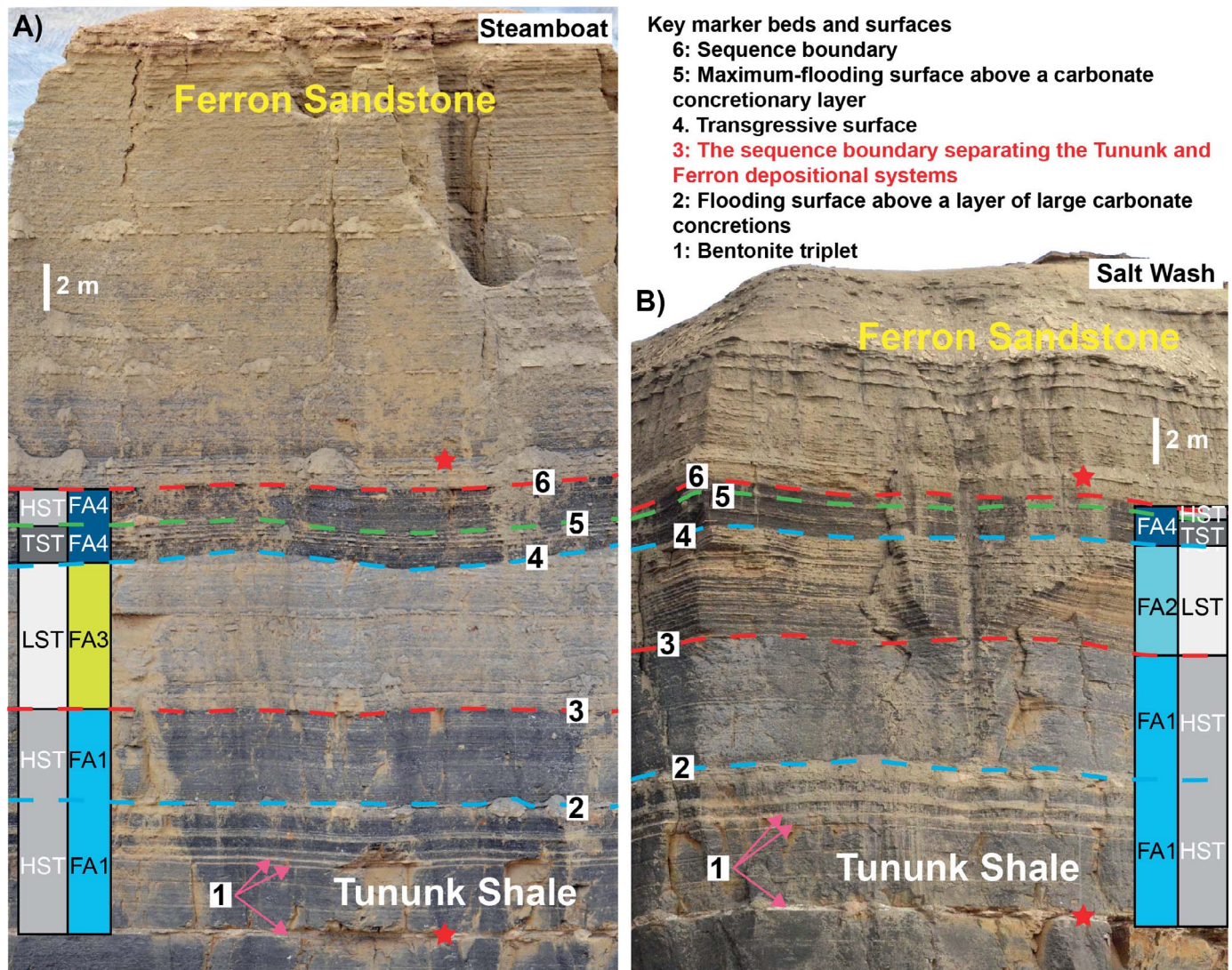
Fig. 11.—Correlation of system tracts present in the studied interval between Steamboat and Salt Wash in outcrops. The stacking of facies associations and system tracts at North Caineville is the same as that at Salt Wash (Fig. 5) and therefore is not shown here. Stars in each photo indicate the extent of measured sections shown in Figure 5. Marker beds or surfaces 1–6 are laterally continuous across our study and therefore serve as reliable chronostratigraphic constraints. Surface 3 represents the T-F sequence boundary, which is overlain by different facies associations between Steamboat vs. Salt Wash and North Caineville. Vertical scales in the two photos are the same. Both photos are strongly contrast-enhanced. The sandstone-rich intervals at the top part of both photos unequivocally belong to the Ferron Sandstone Member in terms of lithology. Nevertheless, the T-F sequence boundary separating the genetic Tununk from Ferron depositional systems (surface 3) is located in a mudstone-dominated interval and can be recognized only based on detailed sedimentary-facies analysis.

Parasequences formed in the prodelta environment (FA3) also commonly show a distinct coarsening-upward facies succession in outcrops (Fig. 10C). The sandstone-to-mudstone ratio distinctly increases upwards in a given parasequence (Fig. 10C). Fine-grained turbidites and hyperpycnites commonly occur in the lower part of a parasequence, and are typically succeeded by thicker and coarser river-flood event deposits (e.g., thick-bedded sandstones showing partial Bouma sequences or soft-sediment deformation) towards the top of a parasequence (Fig. 5).

Parasequences in FA4 are more challenging to recognize in outcrop, due to its dominant fine grain size and subtle grain-size variation. When examined closely, thin beds of coarse mudstone or very fine sandstone that show wave-ripple lamination tend to increase upward in an FA4 parasequence (Fig. 10D). Because FA1, FA2, and FA4 were all interpreted to be deposited in the storm-dominated inner-shelf environment, the upward-shallowing trend of parasequences in these facies associations is

reflected by the upward increase in the frequency and thickness of sandstone beds showing wave-ripple lamination (Figs. 5, 10).

In all four facies associations, features like well-cemented layers, carbonate-concretion layers, the concentrations of volcanic ash, fossil fragments, or phosphatic particles usually occur very close to, or directly below, flooding surfaces (Figs. 5, 10). These features can help identify flooding surfaces because they are commonly formed during periods of sediment starvation (low clastic dilution, low sedimentation rate, or constant winnowing by bottom currents) during rapid sea-level rise (Kidwell 1986; Loutit et al. 1988; Macquaker and Taylor 1996; Taylor and Macquaker 2014; Li and Schieber 2015; Föllmi 2016). The recognition of flooding surfaces based solely on any one of these features, however, may be erroneous because 1) volcanic eruptions may not always coincide with flooding events in time, 2) the concentration of fossil fragments or phosphatic particles can also be generated by a single extreme storm event,

and 3) carbonate concretions can also form during periods of sediment bypass associated with base-level fall (Föllmi 2016). Therefore, the co-occurrence of those features, along with whether the sedimentary facies below and above these features show abrupt changes needs to be considered to ensure the accurate recognition of parasequence boundaries (i.e., flooding surfaces) in offshore mudstone-dominated successions.

Systems Tracts

Based on stacking patterns, parasequences recognized in each measured section can be grouped into different systems tracts that can be correlated across our study area (Figs. 5, 11). The basal interval of all three measured sections comprises FA1 deposited in a medial inner-shelf environment. FA1 parasequences constitute a highstand system tract (HST) that represents the final stage of Tunuk deposition (HST of sequence 4 in Li and Schieber 2020). A sequence boundary is recognized at the top of FA1 in all measured sections (surface 3 in Fig. 11). At Salt Wash and North Caineville FA1 is overlain by FA2, while at Steamboat FA1 is overlain by FA3 (Figs. 5, 11). The surface on top of FA1 in all three localities is recognized as a sequence boundary based on erosional truncation below and onlap above (Fig. 5), and the abrupt basinward shift in sedimentary facies associations across this surface (from medial-inner-shelf FA1 to proximal-inner-shelf FA2 or river-dominated prodelta FA3).

FA4 occupies the uppermost part of the studied interval, overlying FA2 at Salt Wash and North Caineville and FA3 at Steamboat (Fig. 9). The base of FA4 is interpreted as a transgressive surface (surface 4 in Fig. 11) because it marks the first abrupt landward shift in sedimentary facies associations, indicative of a rapid relative rise of sea level. FA2 or FA3, between FA1 and FA4, therefore represent the lowstand system tract (LST) at Salt Wash–North Caineville and Steamboat, respectively.

FA4 can be further divided into a transgressive system tract (TST) and a highstand system tract (HST; Fig. 9). The distinctly high content of fossil fragments and phosphatic particles indicate that FA4 was deposited during a period of minimum clastic dilution, probably due to the rapid rise of sea level (transgression). The maximum flooding surface in FA4 (surface 5 in Fig. 11) is recognized based on the minimum amount of (wave-rippled) silty and sandy laminae (Fig. 5). FA4 in all three measured sections is capped by another sequence boundary (surface 6 in Fig. 11), similar in character to the T-F sequence boundary on top of FA1.

The T-F Sequence Boundary That Separates the Tunuk and Ferron Systems

The sequence boundary on top of FA1 is an unconformity resulting from erosion or nondeposition, as evidenced by erosional truncation below and onlap above (Fig. 5). It is designated as the T-F sequence boundary because it separates the genetic Tunuk from Ferron depositional systems and marks the time when the Ferron Notom delta started to influence the study area. At Steamboat, the T-F sequence boundary is characterized by a sharp surface that separates FA3 from the underlying FA1 (Figs. 11), indicating a sudden increase in sedimentation rate and basinward shift of depositional environments from medial inner shelf to prodelta. The predominance of sedimentary structures generated by river-dominated flood processes, as well as abundant land-plant debris, in FA3 are direct evidence of the influence of the ancient Ferron Notom delta, which prograded from southwest of our study area (Fig. 1B). Therefore, The T-F sequence boundary separates the last HST in the Tunuk system from the first LST in the Ferron system composed of FA1 and FA3, respectively (Fig. 11).

In outcrops, the T-F sequence boundary at Steamboat is characterized by an abrupt change from gray FA1 to overlying light gray FA3 (Figs. 11A, 12A). The overall grayish color of FA1 is due to common to complete bioturbation, which mixed sand and coarse mud particles with fine mud particles (Fig. 6E, F), whereas the light gray color of FA3 is due to a distinctly greater coarse silt content, likely supplied by the distributary channels of the Notom delta. The T-F sequence boundary at Steamboat is overlain by an ~ 3 cm coarse mudstone bed that shows normal grading and wave-ripple lamination (Fig. 12A, B). The T-F sequence boundary is locally capped by a thin (< 500 μm) lag layer of fine-sand-size quartz, carbonate particles (dolomite and calcite), and phosphatic grains in polished slabs and thin section (Fig. 12B–D). Petrographic examination indicates that dolomite grains are present only in FA3 but are absent in FA1, indicating that they are of detrital origin and were derived from hinterland erosion. Dolomite has not been observed anywhere in the Tunuk Shale (Li and Schieber 2018b), hence its presence in FA3 above the T-F sequence boundary indicates that the shift from the Tunuk to Ferron depositional system is accompanied by distinct changes in provenance. This is yet another strong piece of evidence that the Tunuk and Ferron depositional systems separated by the T-F sequence boundary are genetically different from each other.

A sequence boundary can also be recognized on top of FA1 at Salt Wash and North Caineville based on the abrupt basinward shift in facies associations. This sequence boundary, however, is overlain by FA2 in these two localities. Based on the chronostratigraphic constraint provided by the bentonite triplet and the condensed mudstone interval (Fig. 11), the sequence boundary separating FA1 and FA2 at Salt Wash and North Caineville is considered the lateral equivalent to the T-F sequence boundary that separates FA1 and FA3 at Steamboat. The equivalent T-F sequence boundary at Salt Wash and North Caineville is much more subtle in outcrops (Fig. 13A), but it is nonetheless a sharp and laterally traceable surface when examined in close detail. At Salt Wash and North Caineville, FA2 above the T-F sequence boundary is distinctly more laminated and much less bioturbated (non- to only slightly bioturbated) compared to the FA1 below (Fig. 11A). The change from FA1 to FA2 across the sequence boundary indicates an abrupt increase in storm frequency and shift in depositional environments from medial inner shelf to proximal inner shelf. Sedimentary structures generated by river-dominated flood processes are mostly absent in FA2.

At Salt Wash and Steamboat, the equivalent T-F sequence boundary is characterized by a subtle color change from gray FA1 below to dark gray FA2 above (surfaces indicated by red arrows in Figs. 11 and 13A). The lighter color of FA1 is due to common to complete bioturbation. The darker color of FA2, however, is likely associated with its well-laminated nature, characterized by the separation of darker-colored intervals rich in fine mud particles from less common light-colored laminae/beds composed of coarse mud to very fine sand. The petrographic composition of FA2 above the SB is overall similar to that of FA1 below the SB. Detrital carbonate particles (dolomite and calcite) present in FA3 at Steamboat are absent in FA2 at Salt Wash and North Caineville (Fig. 13B–D).

DISCUSSION

Cause of the T-F Sequence Boundary and Its Lateral Variability

The T-F sequence boundary in all three measured sections is interpreted as produced by an allogenic base-level fall (e.g., sea-level fall). Although the abrupt change from FA1 (medial inner shelf) to FA3 (prodelta) at Steamboat can also be generated by autogenic avulsion of a delta lobe, autogenic processes can be ruled out by considering the characteristics of the equivalent T-F sequence boundary at Salt Wash and North Caineville, which separates FA2 from the underlying FA1. The T-F sequence boundary at Salt Wash and North Caineville cannot be attributed to the lateral avulsion of a delta lobe because 1) both FA1 and FA2 are interpreted as deposited under dominant storm influence without fluvial influence and 2) their differences reflect changes in water depth rather than proximity to a river mouth. Therefore, the T-F sequence boundary at Steamboat, Salt Wash, and North Caineville is attributed to the same base-level fall event.
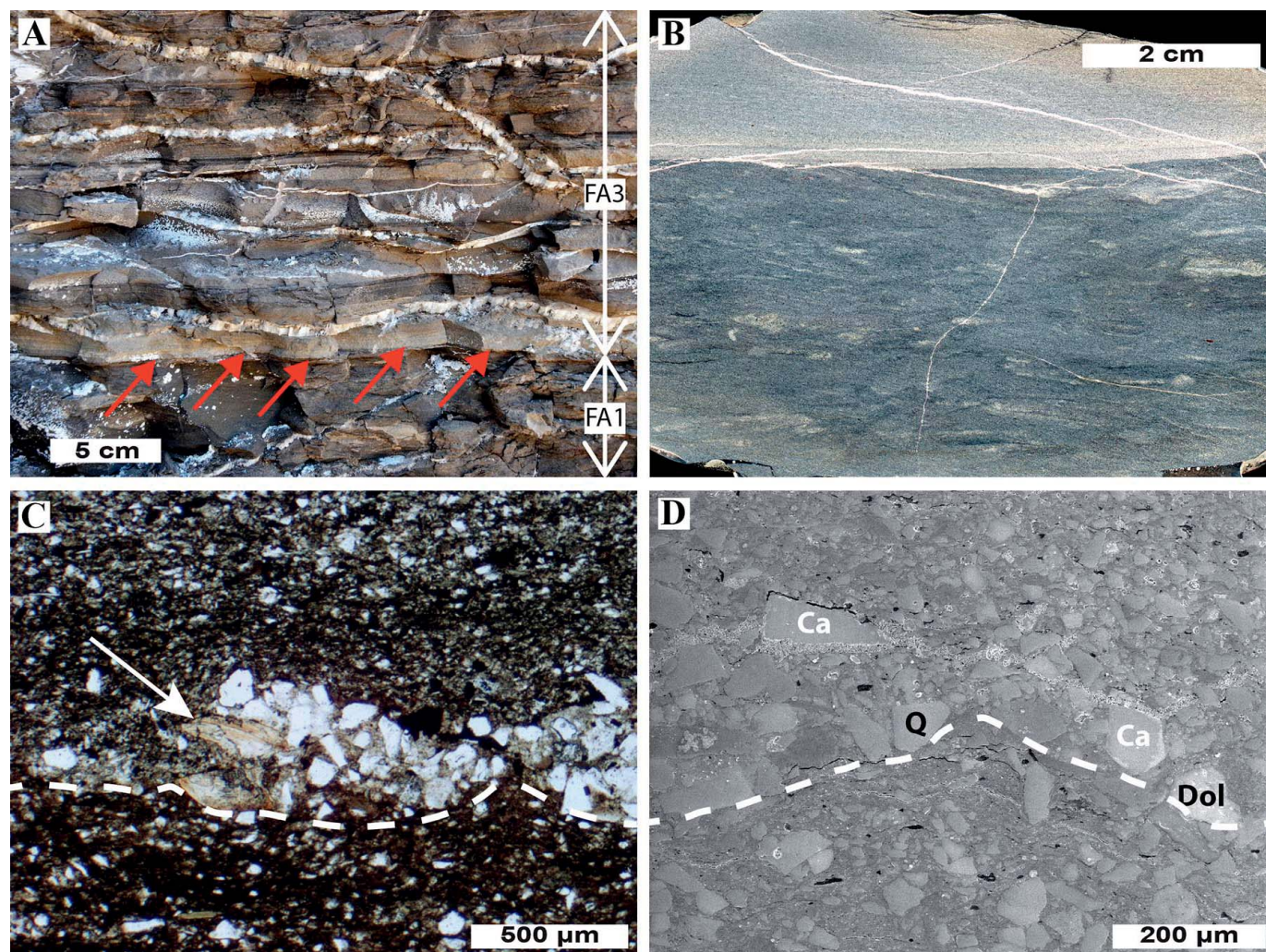
FIG. 12.—Characteristics of the T-F sequence boundary at Steamboat. **A)** The T-F sequence boundary is characterized by a sharp surface (indicated by red arrows) in outcrop. The T-F sequence boundary separates FA1 from FA3 and is overlain by an ~ 3-cm-thick coarse mudstone bed showing normal grading and wave-ripple lamination (note symmetrical ripple crest). **B)** Scanned and processed images of a polished slab of a sample across the T-F sequence boundary. The T-F sequence boundary separates the highly bioturbated medium mudstone (FA1) from the overlying rarely bioturbated coarse mudstone (FA3). **C)** Photomicrograph (plane-polarized light) showing that the T-F sequence (white dashed line) is overlain by a thin (< 500 μm) lag layer made of very fine sand-size siliciclastic particles and fossil fragments (white arrow). **D)** SEM photomicrograph (secondary electron mode) of an area close to the area in Part C showing that the lag layer consists of both siliciclastic and carbonate particles. The T-F sequence boundary is indicated by the white dashed line. Q, quartz; Ca, calcite; Dol, dolomite.

Dominant sedimentary structures generated by river floods (fine-grained turbidites and hyperpycnites) in the first Ferron LST (Fig. 8) indicate that during the deposition of FA3 Steamboat was located close (within 50 km; Bohacs et al. 2014) to the river mouth or the distributary-channel system of the proto–Notom delta. When base level fell, the river mouth of the Notom delta prograded farther towards the Steamboat area, leading to greater terrigenous input and increased frequency and magnitude of river-flood events (Fig. 1B), and formation of an erosional surface and a thin (< 500 μm) lag layer (Fig. 12). The coarse mudstone bed directly overlying the T-F sequence boundary at Steamboat (Fig. 10A) is interpreted as deposited from storm-influenced or storm-enhanced surge-type turbidity currents or hyperpycnal flows based on the presence of detrital dolomite grains (directly supplied by the river), normal grading, and wave-ripple lamination (Lamb et al. 2008; Macquaker et al. 2010; Li et al. 2015). The T-F sequence boundary at Steamboat is therefore a subaqueous unconformity formed by erosion of the sea bottom by river floods and storm events at shallower water depth.

At Salt Wash and North Caineville, the equivalent T-F sequence boundary is characterized by an abrupt juxtaposition of FA2 over FA1. The distinct increase in the abundance and lateral continuity of storm-generated sedimentary features, as well as the decrease in BI, suggests increased frequency or magnitude of storm events during the deposition of FA2 compared to FA1 (assuming each parasequence was deposited over a similar time span). Therefore, the T-F sequence boundary at Salt Wash and North Caineville represents a subaqueous unconformity due to more frequent storm erosion and reworking of the seabed on a shallower storm-dominated shelf.

Different expressions of the T-F sequence boundary and its lateral equivalent at Steamboat vs. Salt Wash and North Caineville are due to different geographical location of these localities relative to the river mouth of the proto–Notom delta system. Steamboat was located closer to the river mouth and received more terrigenous sediment and was subject to more energetic river-dominated (and storm-influenced) processes after base level fell. The thin lag layer associated with the T-F sequence boundary at
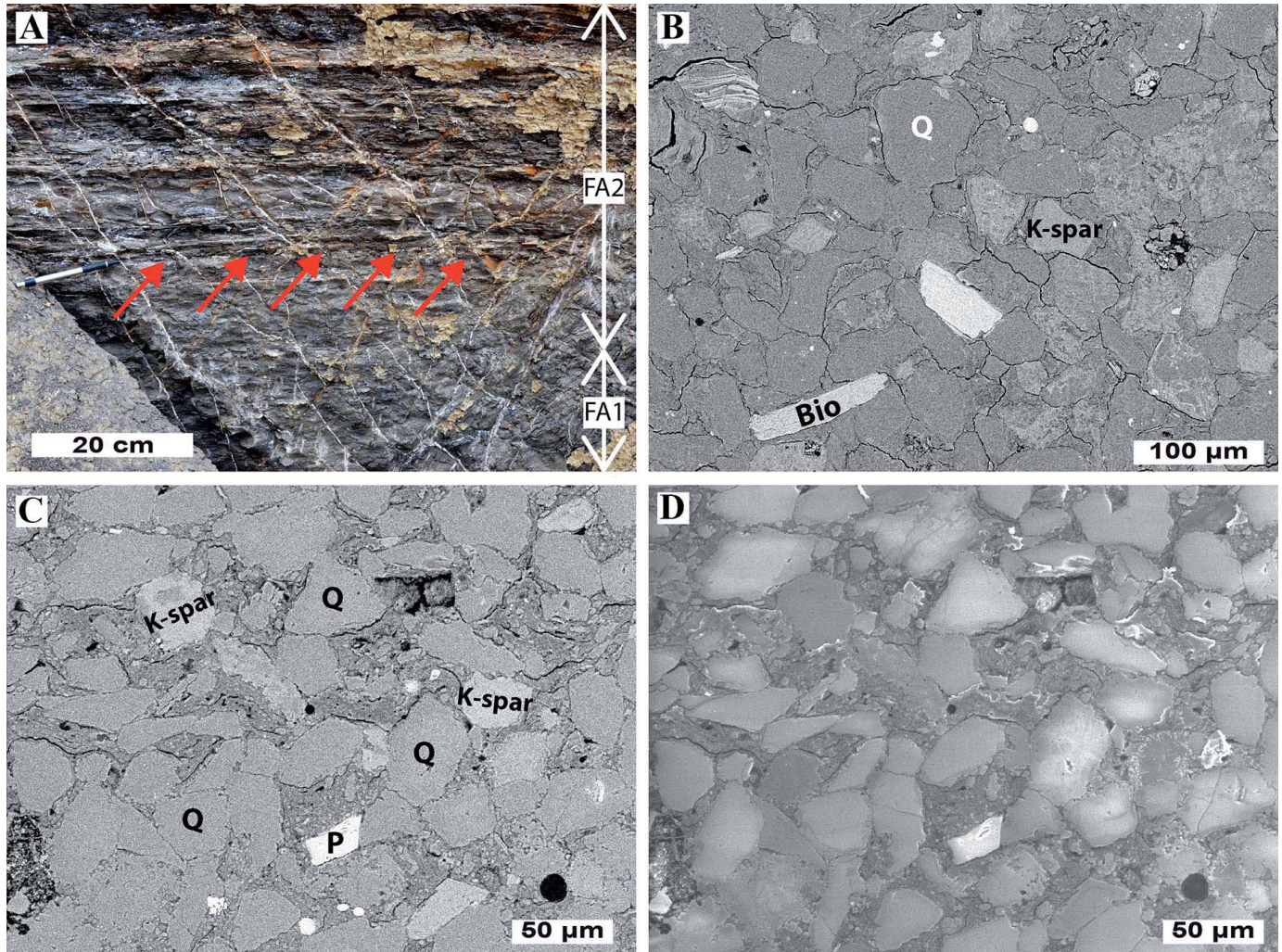
Fig. 13.—Characteristics of the T-F sequence boundary at Salt Wash. **A)** The T-F sequence boundary is much more subtle (indicated by red arrows) in outcrop. Note that the FA1 below the T-F sequence boundary appears more homogeneous, whereas the overlying FA2 is distinctly more interbedded. Due to difficulties in collecting samples containing the T-F sequence boundary, only samples below and above the T-F sequence boundaries were collected. **B)** SEM photomicrograph (backscatter mode) showing that the FA1 sample below the T-F sequence boundary contains mostly siliciclastic minerals (quartz, feldspar, biotite, and clay minerals). **C**, **D)** SEM photomicrographs (backscatter and secondary electron mode) of the same area showing that the FA2 sample above the T-F sequence boundary is characterized by almost the same petrographic compositions as FA1. FA2 does not contain detrital carbonate particles (no particles in Part D show charging effect). Q, quartz; K-spar, potassium feldspar; Bio, biotite; P, apatite.

Steamboat (Fig. 12B) indicates reworking and concentration of incoming coarser terrigenous particles (e.g., detrital carbonate particles) by river-generated turbidity currents or storms during the base-level fall. Meanwhile, Salt Wash and North Caineville were still located in a storm-dominated shelf environment without direct fluvial influence. Thin-section petrography shows no distinct compositional differences between FA1 and FA2, indicating that sediment provenance did not change significantly across the T-F sequence boundary at Salt Wash and North Caineville (Fig. 13). Instead, the decreased water depth led to a change in the textural arrangement of fine-grained vs. coarser-grained sediment particles. Below the T-F sequence boundary, lower sedimentation rates associated with slightly deeper water during the last Tununk HST are manifested through common disruption of primary sedimentary features and textural homogenization by bioturbation in FA1 (Fig. 13). Above the T-F sequence boundary, fine mud and coarse mud to very fine sand are well segregated into distinct layers in FA2 due to more frequent storm events and minimal BI during shallower water depth (Fig. 7).

The presence and absence of detrital dolomite in FA3 and FA2, respectively, provides another piece of evidence of different depositional settings between Steamboat vs. Salt Wash–North Caineville. Paleogeographic reconstructions indicate that the source area of the Ferron Notom delta was located southwest of our study area (Fig. 1B), where thrust sheets in southern Utah exposed Proterozoic through Mesozoic quartzites, sandstones, and carbonate rocks (Szwarc et al. 2015). The absence of dolomite grains in FA1 indicates that during deposition of the Tununk Shale, the proto–Notom delta had not yet prograded to the Henry Mountains region and thus could not supply detrital carbonate particles to the Tununk depositional system when base level was high. An additional reason for the Tununk–Ferron provenance difference is that the Tununk Shale was deposited as an offshore mud belt, with sediment supply largely from north of our study area by south-directed geostrophic currents (Li and Schieber 2018a). The absence of dolomite grains in FA2 indicates the southward-directed longshore currents prevented sediments from the river

mouth from being dispersed northward because Salt Wash and North Caineville were located updrift of Steamboat (Figs. 1, 4).

The presumed different proximity of the three study localities to the river mouth in the proto–Notom delta system is also supported by variations in the thickness of certain system tracts in the studied interval. Among all three measured sections, the interval between the bentonite triplet and the T-F sequence boundary (Tununk HST) is the thinnest, whereas the interval between the T-F sequence boundary and the condensed mudstone interval (Ferron LST to HST) is the thickest at Steamboat (Fig. 5). The thin Tununk HST at Steamboat (closest to the river mouth) reflects the higher erosional capability of frequent surge-type turbidity currents and hyperpycnal flows (potentially aided or enhanced by storms), consistent with the observation of a thin lag layer and the truncation of at least one or two parasequences below the T-F sequence boundary at Steamboat (Fig. 5). The larger erosion associated with the T-F sequence boundary at Steamboat resulted in additional accommodation, reflected by the onlap against the T-F sequence boundary away from Steamboat (Fig. 5). This larger accommodation, combined with higher sedimentation rates due to abundant terrigenous input close to the river mouth, led to the thickest Ferron LST occurring at Steamboat.

Correlative Conformity or Subtle Unconformity?

In all measured sections, the T-F sequence boundary occurs in a mudstone-dominated interval and is characterized by a mudstone-on-mudstone contact, much more subtle in nature when compared to "classical" sequence boundaries observed in more proximal environments. The T-F sequence boundary marking the onset of the Ferron Notom delta system at Steamboat can be identified only on the basis of sedimentary facies and petrographic characteristics across this surface. At Salt Wash and North Caineville, the sequence boundary is defined by even more subtle variations in grain size and sedimentary-facies characteristics (Fig. 13). To the authors' knowledge, there is to date no published study in which a "correlative conformity" in distal shelf mudstones has been identified in a ramp or shelf setting on the basis of detailed examination of sedimentologic and petrographic characteristics. This state of affairs is probably rooted in dated assumptions with regard to the nature of correlative conformities. If sequence boundaries in distal shelf environments were indeed (correlative) conformities, objective criteria to locate them in outcrops or cores would be lacking (Embry 2002). However, in this study none of the T-F sequence boundaries documented in the measured sections are true conformities. The slightly undulatory erosional surface and thin lag layer (Fig. 12), as well as the erosional truncation below and onlap above (Fig. 5), suggest that the T-F sequence boundary at Steamboat is a subaqueous unconformity that represents an erosional and nondepositional hiatus. The abrupt juxtaposition of proximal inner-shelf facies on top of medial-shelf facies, the clear contrast between FA1 and FA2 (only "clear" after detailed sedimentologic facies analysis), and interpreted onlap relations (Fig. 5), all suggest that the T-F sequence boundary at Salt Wash and North Caineville still represents some degree of hiatus and therefore is not a true conformity.

The T-F sequence boundary thus represents a subtle unconformity. When sequence boundaries were originally defined based on seismic stratigraphy, only surfaces that represent hiatuses "encompassing a significant interval of geologic time" were considered as unconformities, and surfaces representing hiatuses of relatively small duration (i.e., subtle unconformities that are below seismic resolution) were not considered an unconformity (Mitchum et al. 1977). The studied interval (from the bentonite triplet to the condensed section) is less than 20 m in thickness, at the resolution limit for conventional seismic profiles (Faleide et al. 2019). Additionally, the two marker beds (i.e., the bentonite triplet and the condensed section) bracketing the T-F sequence boundary are laterally continuous across our study area (over an area of at least 30 km by 30 km).

Even though the T-F sequence boundary can be documented as characterized by erosional truncation below and onlap above based on high-resolution stratigraphic correlation (Fig. 5), it would likely be categorized as a correlative conformity because the associated stratal termination is only at meter scale (Fig. 5), unlikely to be resolved in seismic data (Mitchum et al. 1977).

The presumption that sequence boundaries in distal marine environments, where the strata are mudstone-dominated, are conformities by default may not be warranted. Historically, this perspective was likely based on the assumption that mudstones generally accumulate via passive setting in low-energy settings, without consideration given to the possibility that they might be eroded again. However, common event beds (e.g., fine-grained turbidites, hyperpycnites, and tempestites) documented in the Tununk–Ferron transition and many other mudstone-dominated successions deposited in distal marine environments indicate that the deposition of offshore muds were subject to a variety of bottom currents with erosion potential (Plint 2014; Wilson and Schieber 2014; Trabucho-Alexandre 2015; Birgenheier et al. 2017; Li and Schieber 2018a). Detailed sedimentologic and petrographic analyses and high-resolution stratigraphic correlation are therefore required to identify changes in depositional conditions, erosion by energetic bottom currents, and hiatus in the record of fine-grained rocks.

Another key feature that sequence stratigraphic models in a shelf or ramp setting (Posamentier et al. 1992; Catuneanu 2006; Neal et al. 2016) fail to consider is the presence of muddy subaqueous clinothems. In our study area, the Tununk Shale was deposited as an offshore mud belt under the combined influence of storm-generated offshore-directed currents and along-shelf geostrophic currents (Li and Schieber 2018a), and likely is analogous to the muddy subaqueous clinoforms that have been documented in a number of modern offshore mud blankets (Leithold 1994; Ridente and Trincardi 2005; Liu et al. 2006; Cattaneo et al. 2007; Li and Schieber 2018a). In contrast, the Ferron Sandstone was deposited as a subaerial delta and thus exhibits subaerial clinothems (Zhu et al. 2012). The T-F sequence boundary documented in this study therefore marks the transition from the Tununk subaqueous clinothem system to the Ferron subaerial clinothem system (Fig. 14). When compared to muddy subaqueous clinothems, sand-prone subaerial clinothems are generally one order of magnitude steeper ($\geq 0.26°$; Pirmez et al. 1998; Patruno et al. 2015; Patruno and Helland-Hansen 2018). The steeper slope and greater wave and current velocities required to transport sand associated with subaerial clinothems is likely the reason for the larger erosion associated with the T-F sequence boundary at Steamboat (Figs. 5, 14A). On a storm-dominated shelf, muddy subaqueous clinoforms typically are very gently dipping (0.01–0.38°) and have wide subaqueous topsets (Patruno et al. 2015). Under those circumstances, even a small-magnitude base-level fall (and associated lowering of wave base) could cause widespread erosion of the subaqueous clinothem topsets (Fig. 14B), leading to the formation of the T-F sequence boundary at Salt Wash and North Caineville. The presented schematic model with more realistic clinothem geometry and foreset slope suggests that under those circumstances base-level fall can indeed lead to subaqueous erosion in distal shelf settings (Fig. 14). Based on the general model presented in Figure 14, the spatial extent and magnitude (how much time is missing) of the subaqueous unconformity in distal shelf environments depends on the magnitude of base-level fall and changes in the equilibrium profile (clinothem geometry and foreset slope) through time.

This study indicates that in a shelf or ramp setting, the sequence boundary in distal shelf environments, where the strata are mudstone-dominated, is likely a subtle unconformity rather than a true conformity. Based on a comprehensive sequence stratigraphic study using different datasets, Miller et al. (2013) found little evidence of a correlative conformity in the distal basinal environment in a shelf–slope setting, because even there, hiatuses of relatively small duration associated with
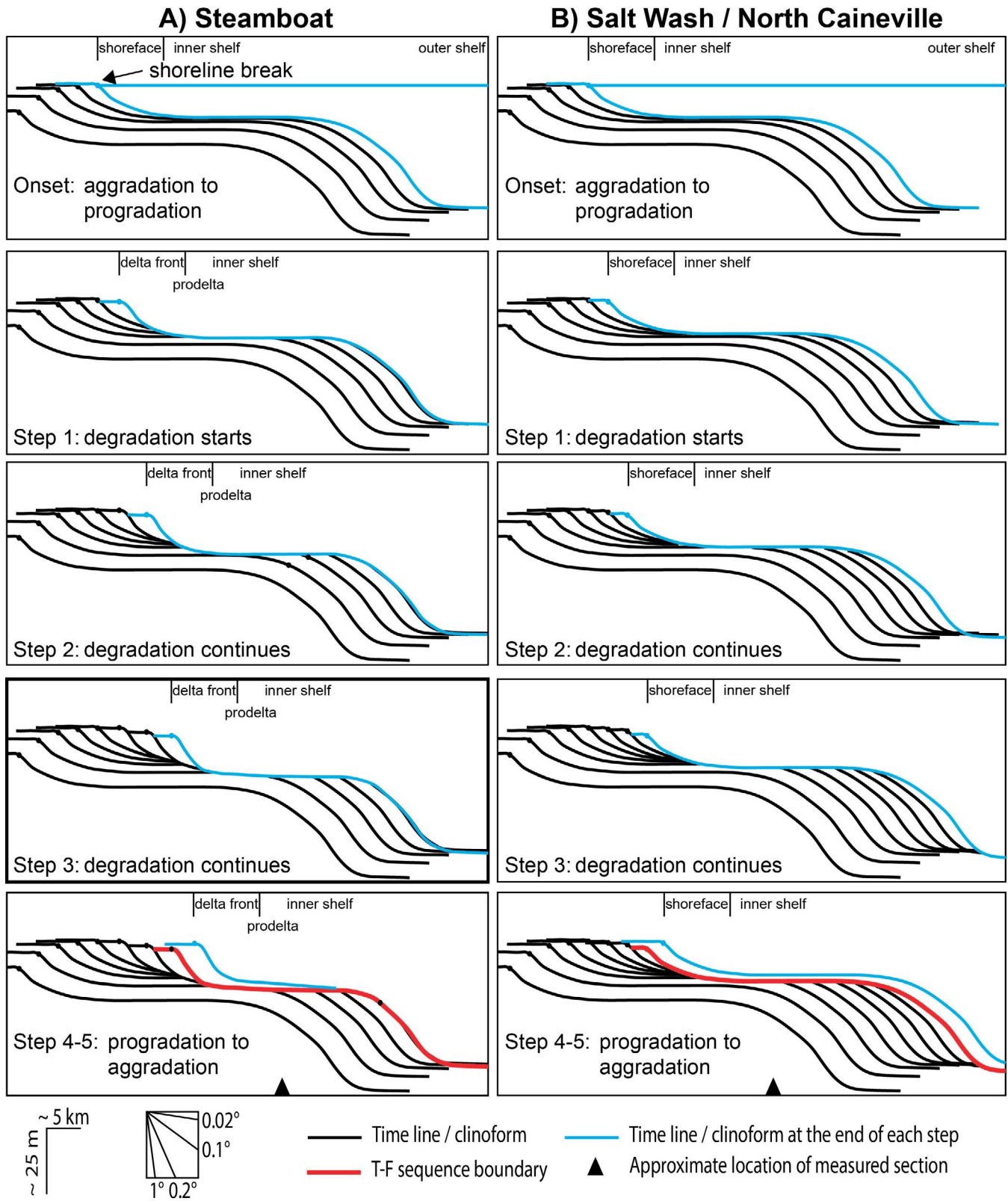
FIG. 14.—Schematic drawing illustrating the formation of the T-F sequence boundary and causes of its lateral variability. Onset: aggradation to progradation during the last Tununk HST. Steps 1–3: degradational stacking pattern resulting from base-level fall. Steps 4–5: progradation to aggradation during the first Ferron LST. The Tununk Shale was deposited as an offshore mud belt, which contains subaqueous clinothems, whereas the Ferron Sandstone was deposited as a delta characterized by subaerial clinoforms. The geometry and slope of subaqueous and subaerial clinothems are based on average values from Patruno et al. (2015). The larger degree of hiatus associated with the T-F sequence boundary at Steamboat is attributed to deeper fair-weather wave base associated with steeper subaerial clinoforms (see text for expanded explanation). The schematic model with more realistic clinoform geometry and slope suggests that a subaqueous unconformity can develop in even distal shelf settings in a ramp setting. The model proposed here assumes that the geometry of the equilibrium profile (each clinothem) stays constant and only changes between subaerial and subaqueous clinothems. The extent of a subaqueous unconformity depends on the magnitude of base-level fall, amount of sediment supply, and changes in the equilibrium profile through time.

sequence boundaries can be identified based on evidence of erosion in core. Therefore, the existence of a correlative conformity remains unproven in basins with or without a shelf break, and the uncritical use of the term "correlative conformity" should be avoided.

Significance of Recognizing Sequence Boundaries in Distal Marine Settings

Based on above considerations, many offshore mudstone-dominated successions, despite their homogeneous appearance, are likely to contain more subtle unconformities than previously considered. Similar to sequence boundaries identified in proximal sandstone-dominated settings, subtle unconformities (i.e., sequence boundaries) can be used to divide shelf mudstone strata into genetically related stratal packages. A better understanding of the sequence stratigraphic framework of mudstone-dominated successions is critical for the correct interpretation of paleoenvironmental changes (e.g., changes in sea level, provenance, and climate) recorded by these rocks.

The accurate recognition of subtle unconformities in distal shelf mudstones can yield critical insights into the timing and mechanism (allogenic vs. autogenic) of past sea-level events. Currently, the reconstruction of past sea-level history depends largely on the sequence boundaries recognized in sandstone-dominated proximal deltaic or shoreline successions (Miller et al. 2004; Amorosi et al. 2017). Yet, because proximal deltaic or shoreline successions are usually associated with significant amounts of erosion, determining the exact timing of sea-level fall can be challenging. In our study, for instance, the bentonite triplet that is used as a time marker across the three measured sections is absent in areas farther southwest (more proximal environments of the proto–Notom delta system) of our study area (Zhu et al. 2012), indicating a larger degree of erosion or nondeposition in the more energetic proximal setting. In addition, sequence boundaries formed in proximal environments can be highly diachronous. The base of incised-valley fills, for instance, although relatively easy to identify in outcrop and core studies, is, in most cases, a composite feature that represents neither a specific topographic surface nor a specific time (Strong and Paola 2008; Bhattacharya 2011; Holbrook and Bhattacharya 2012). In contrast, as shown in this study, subtle unconformities formed in distal (i.e., below fair-weather wave base) mudstone-dominated successions are associated with erosional or non-depositional hiatuses of shorter duration than their proximal counterpart—the exact reason why sequence-bounding unconformities detected at the basin margin often lose seismic expression when traced basinward. These distal erosional surfaces are produced by bottom currents whose frequency and magnitude depend largely on water depth and are therefore characterized by a much more subdued topographic relief. Because the associated hiatuses are comparatively minor, sequence boundaries in distal marine environments may be much better suited to constrain the timing of sea-level events. Additionally, features such as fossil fragments and bentonite marker beds are also more likely preserved in distal shelf mudstones, providing tighter chronostratigraphic constraints for the base-level event. For instance, the topmost bentonite bed of the bentonite triplet was dated as 90.64 ± 0.25 Ma based on $^{40}Ar/^{39}Ar$ isotopic dating (Zhu et al. 2012), providing a maximum age for the base-level fall event represented by the T-F sequence boundary.

The along-shelf lateral variability in the characteristics of the distal sequence boundary is another important topic largely overlooked in previous studies. The correlation of the T-F sequence boundary with excellent chronostratigraphic constraints across the study area is critical to correctly dividing mudstones into genetically related packages. If only examining the T-F transition at Salt Wash or North Caineville, it is almost impossible to identify the boundary between FA1 and FA2 as the sequence boundary that separates the genetic Tununk from the Ferron system at these two localities. Neither detailed sedimentologic facies analysis nor

petrographic analysis can provide any direct evidence suggesting that the onset of the Ferron system occurred across the boundary between FA1 and FA2 because both facies associations reflect deposition on a storm-dominated shelf without direct fluvial influence. However, careful correlations with the age-equivalent interval at Steamboat with reliable physical stratigraphic constraints (i.e., ash beds and condensed section) indicate that FA2 was deposited updrift of FA3 during the same time interval and therefore is genetically related to the Ferron depositional system. Thus, the sequence boundary on top of FA1 at Salt Wash and North Caineville is indeed the lateral equivalent of the T-F sequence boundary recognized at Steamboat. This has critical implications into sequence stratigraphic correlations along depositional strike—laterally equivalent sequence stratigraphic surfaces may be characterized by different juxtapositions of facies associations (i.e., depositional environments). In addition to vertical variations in facies variations, reliable physical chronostratigraphic constraints are required to strengthen the validity of sequence stratigraphic correlations.

The lateral variability of the characteristics of distal sequence boundaries can yield additional insights into the causes of base-level events recorded in offshore mudstone-dominated successions. Based on comparison between areas directly off and updrift of the river mouth (Steamboat vs. Salt Wash and North Caineville), the T-F sequence boundary is interpreted as due to an allogenic base-level fall because the facies change from FA1 to FA2 and from FA1 to FA3 indicates a relative decrease in water depth. Autogenic processes can be ruled out because the lateral avulsion of a delta lobe cannot produce a sharp surface separating FA1 and FA2, both recording mostly storm influence and absence of fluvial influence, at Salt Wash and North Caineville. Tectonic processes, which are typically long-term processes that influence a broad region, can also be ruled out because the T-F sequence boundary is associated with a rather small hiatus (no biozone is missing). Careful examination of lateral variability of subtle unconformities in shelf mudstone successions can therefore help to identify the dominant process responsible for the formation of the sequence boundary.

CONCLUSIONS

Based on detailed sedimentologic and petrographic analysis combined with careful stratigraphic correlations with excellent chronostratigraphic constraints, the sequence boundary separating the genetic Tununk from the Ferron depositional systems (T-F sequence boundary) can be pinpointed. The T-F sequence boundary marks the change from the Tununk offshore mud-belt system to the Ferron Notom delta system in our study area. Although the T-F sequence boundary occurs in distal offshore environments (below fair-weather wave base) and is characterized by a mudstone-on-mudstone contact, it can be documented as a subtle subaqueous unconformity based on distinct erosional features, abrupt juxtaposition of facies associations indicative of a basinward shift in facies, and lapout relationships (erosional truncation below and onlap above). The T-F sequence boundary varies in character across our study area. In areas directly off the river mouth of the Ferron Notom delta during its earliest stage of development (Steamboat), the T-F sequence boundary is characterized by a sharp and erosional surface overlain by a thin lag layer. In areas away from the river mouth (Salt Wash and Steamboat), the T-F sequence boundary becomes much more subtle. The different expressions of the T-F sequence boundary across our study area are mainly due to different locations relative to the river mouth of the proto–Notom delta. High-resolution correlations of the T-F sequence boundary with reliable chronostratigraphic constraints indicate surfaces characterized by the same facies variation pattern along depositional strike (e.g., parallel to the shoreline orientation) may not be laterally equivalent, and should be correlated only with additional chronostratigraphic constraints.

The uncritical use of the term "correlative conformity" should be avoided. When examined in close detail, offshore mudstone strata appear to contain more subtle unconformities than previously considered. The accurate recognition of sequence boundaries in shelf mudstone successions is critical to dividing such homogeneous-appearing successions into genetically related packages and to facilitating a better utilization of these rocks as important paleoenvironmental archives. Detailed examinations of subtle unconformities in shelf mudstone successions and careful examinations of their lateral variability in characteristics can yield critical insights into the timing and mechanism (allogenic vs. autogenic) of relative changes of sea level recorded in these rocks.

REFERENCES

AINSWORTH, R.B., AND PATTISON, S.A.J., 1994, Where have all the lowstands gone? Evidence for attached lowstand systems tracts in the Western Interior of North America: Geology, v. 22, p. 415–418.

AMOROSI, A., BRUNO, L., CAMPO, B., MORELLI, A., ROSSI, V., SCARPONI, D., HONG, W., BOHACS, K.M., AND DREXLER, T.M., 2017, Global sea-level control on local parasequence architecture from the Holocene record of the Po Plain, Italy: Marine and Petroleum Geology, v. 87, p. 99–111.

APLIN, A.C., AND MACQUAKER, J.H.S., 2011, Mudstone diversity: origin and implications for source, seal, and reservoir properties in petroleum systems: American Association of Petroleum Geologists, Bulletin, v. 95, p. 2031–2059.

AYRANCI, K., HARRIS, N.B., AND DONG, T., 2018, High resolution sequence stratigraphic reconstruction of mud-dominated systems below storm wave base: a case study from the Middle to Upper Devonian Horn River Group, British Columbia, Canada: Sedimentary Geology, v. 373, p. 239–253.

BHATTACHARYA, J.P., 2011, Practical problems in the application of the sequence stratigraphic method and key surfaces: integrating observations from ancient fluvial–deltaic wedges with Quaternary and modelling studies: Sedimentology, v. 58, p. 120–169.

BHATTACHARYA, J.P., AND MACEACHERN, J.A., 2009, Hyperpycnal rivers and prodeltaic shelves in the Cretaceous seaway of North America: Journal of Sedimentary Research, v. 79, p. 184–209.

BHATTACHARYA, J.P., AND TYE, R.S., 2004, Searching for modern Ferron analogs and application to subsurface interpretation, in Chidsey, T.C., Jr., Adams, R.D., and Morris, T.H., eds., The Fluvial–Deltaic Ferron Sandstone: Regional to Wellbore-Scale Outcrop Analogs Studies and Application to Reservoir Modeling: American Association of Petroleum Geologists, Studies in Geology, v. 50, p. 39–57.

BHATTACHARYA, J.P., HOWELL, C.D., MACEACHERN, J.A., AND WALSH, J.P., 2020, Bioturbation, sedimentation rates, and preservation of flood events in deltas: Palaeogeography, Palaeoclimatology, Palaeoecology, v. 560, no. 110049.

BIRGENHEIER, L.P., HORTON, B., MCCAULEY, A.D., JOHNSON, C.L., AND KENNEDY, A., 2017, A depositional model for offshore deposits of the lower Blue Gate Member, Mancos Shale, Uinta Basin, Utah, USA: Sedimentology, v. 64, p. 1402–1438.

BLAKEY, R.C., 2014, Paleogeography and Paleotectonics of the Western Interior Seaway, Jurassic–Cretaceous of North America: American Association of Petroleum Geologists, Search and Discovery Article #30392, 72 p.

BOHACS, K.M., 1998, Contrasting expressions of depositional sequences in mudrocks from marine to non-marine environs, in Schieber, J., Zimmerle, W., and Sethi, P.S., eds., Shales and Mudstones: Stuttgart, Schweizerbart'sche Verlagsbuchhandlung, p. 33–78.

BOHACS, K.M., AND SCHWALBACH, J.R., 1992, Sequence stratigraphy of fine-grained rocks with special reference to the Monterey Formation, in Schwalbach, J.R., and Bohacs, K., eds., Sequence Stratigraphy in Fine-Grained Rocks: Examples from the Monterey Formation: SEPM, Pacific Section, Field Trip Guidebook, v. 70, p. 7–19.

BOHACS, K.M., NEAL, J.E., GRABOWSKI, G.J., JR., ARMENTROUT, J.M., AND ROSEN, N.C., 2002, Sequence stratigraphy in fine-grained rocks: beyond the correlative conformity, in Armentrout, J.M., and Rosen, N.C., eds., Sequence Stratigraphic Models for Exploration and Production: Evolving Methodology, Emerging Models and Application Histories: SEPM, Gulf Coast Section, 22nd Annual Bob F. Perkins Research Conference, p. 130–136.

BOHACS, K.M., GRABOWSKI, G.J., JR., CARROLL, A.R., MANKIEWICZ, P.J., MISKELL-GERHARDT, K.J., SCHWALBACH, J.R., WEGNER, M.B., AND SIMO, J.A., 2005, Production, destruction, and dilution: the many paths to source-rock development, in Harris, N., eds., The Deposition of Organic Carbon-Rich Sediments: Mechanisms, Models and Consequences: SEPM, Special Publication 82, p. 61–101.

BOHACS, K.M., LAZAR, O.R., AND DEMKO, T.M., 2014, Parasequence types in shelfal mudstone strata: quantitative observations of lithofacies and stacking patterns, and conceptual link to modern depositional regimes: Geology, v. 42, p. 131–134.

CAMPBELL, C.V., 1967, Lamina, laminaset, bed and bedset: Sedimentology, v. 8, p. 7–26.

CATTANEO, A., TRINCARDI, F., ASIOLI, A., AND CORREGGIARI, A., 2007, The western Adriatic shelf clinoform: energy-limited bottomset: Continental Shelf Research, v. 27, p. 506–525.

CATUNEANU, O., 2006, Principles of Sequence Stratigraphy: Amsterdam, Elsevier Science, 375 p.

CATUNEANU, O., 2019, Model-independent sequence stratigraphy: Earth-Science Reviews, v. 188, p. 312–388.

CATUNEANU, O., ABREU, V., BHATTACHARYA, J.P., BLUM, M.D., DALRYMPLE, R.W., ERIKSSON, P.G., FIELDING, C.R., FISHER, W.L., GALLOWAY, W.E., GIBLING, M.R., GILES, K.A., HOLBROOK, J.M., JORDAN, R., KENDALL, C.G.S.C., MACURDA, B., MARTINSEN, O.J., MIALL, A.D., NEAL, J.E., NUMMEDAL, D., POMAR, L., POSAMENTIER, H.W., PRATT, B.R., SARG, J.F., SHANLEY, K.W., STEEL, R.J., STRASSER, A., TUCKER, M.E., AND WINKER, C., 2009, Towards the standardization of sequence stratigraphy: Earth-Science Reviews, v. 92, p. 1–33.

ELDER, W.P., AND KIRKLAND, J.I., 1994, Cretaceous paleogeography of the southern Western Interior region, in Peterson, J.A., and Franczyk, K.J., eds., Mesozoic Systems of the Rocky Mountain Region, USA: SEPM, Rocky Mountain Section, p. 415–440.

EMBRY, A.F., 2002, Transgressive–regressive (TR) sequence stratigraphy, in Armentrout, J., and Rosen, N., eds., Sequence Stratigraphic Models for Exploration and Production: Evolving Methodology, Emerging Models, and Application Histories: Gulf Coast Association of Geological Societies, Transactions, Proceedings, v. 52, p. 151–172.

ERICKSEN, M.C., AND SLINGERLAND, R.L., 1990, Numerical simulations of tidal and wind-driven circulation in the Cretaceous Interior Seaway of North America: Geological Society of America, Bulletin, v. 102, p. 1499–1516.

FALEIDE, T.S., MIDTKANDAL, I., PLANKE, S., CORSERI, R., FALEIDE, J.I., SERCK, C.S., AND NYSTUEN, J.P., 2019, Characterisation and development of Early Cretaceous shelf platform deposition and faulting in the Hoop area, southwestern Barents Sea: constrained by high-resolution seismic data: Norwegian Journal of Geology, v. 99, p. 1–20.

FÖLLMI, K.B., 2016, Sedimentary condensation: Earth-Science Reviews, v. 152, p. 143–180.

GARDNER, M.H., 1995, Tectonic and eustatic controls on the stratal architecture of Mid-Cretaceous stratigraphic sequences, central western interior foreland basin of North America, in Dorobek, S.L., and Ross, G.M., eds., Stratigraphic Evolution of Foreland Basins: SEPM, Special Publication 52, p. 243–282.

HEATH, G.R., 1977, Organic carbon in deep-sea sediments, in Andersen, N.R., and Malahoff, A., eds., The Fate of Fossil Fuel CO_2 in the Oceans: Plenum Press, p. 605–625.

HOLBROOK, J.M., AND BHATTACHARYA, J.P., 2012, Reappraisal of the sequence boundary in time and space: case and considerations for an SU (subaerial unconformity) that is not a sediment bypass surface, a time barrier, or an unconformity: Earth-Science Reviews, v. 113, p. 271–302.

KAUFFMAN, E.G., 1985, Cretaceous evolution of the Western Interior Basin of the United States, in Pratt, L.M., Kauffman, E.G., and Zelt, F.B., eds., Fine-Grained Deposits and Biofacies of the Cretaceous Western Interior Seaway: Evidence of Cyclic Sedimentary Processes: SEPM, Field Trip Guide, v. 4, p. iv–xiii.

KEMP, D.B., FRASER, W.T., AND IZUMI, K., 2018, Stratigraphic completeness and resolution in an ancient mudrock succession: Sedimentology, v. 65, p. 1875–1890.

KIDWELL, S.M., 1986, Models for fossil concentrations: paleobiologic implications: Paleobiology, v. 12, p. 6–24.

KORUS, J.T., AND FIELDING, C.R., 2017, Hierarchical architecture of sequences and bounding surfaces in a depositional-dip transect of the fluvio-deltaic Ferron Sandstone (Turonian), southeastern Utah, USA: Journal of Sedimentary Research, v. 87, p. 897–920.

LAGRANGE, M.T., KONHAUSER, K.O., CATUNEANU, O., HARRIS, B.S., PLAYTER, T.L., AND GINGRAS, M.K., 2020, Sequence stratigraphy in organic-rich marine mudstone successions using chemostratigraphic datasets: Earth-Science Reviews, v. 203, p. 103137.

LAMB, M., MYROW, P., LUKENS, C., HOUCK, K., AND STRAUSS, J., 2008, Deposits from wave-influenced turbidity currents: Pennsylvanian Minturn Formation, Colorado, USA: Journal of Sedimentary Research, v. 78, p. 480–498.

LAZAR, O.R., 2007, Redefinition of the New Albany Shale of the Illinois basin: an integrated, stratigraphic, sedimentologic, and geochemical study [Ph.D. Thesis]: Indiana University, 362 p.

LAZAR, O.R., BOHACS, K.M., MACQUAKER, J.H.S., SCHIEBER, J., AND DEMKO, T.M., 2015, Capturing key attributes of fine-grained sedimentary rocks in outcrops, cores, and thin sections: nomenclature and description guidelines: Journal of Sedimentary Research, v. 85, p. 230–246.

LEITHOLD, E.L., 1994, Stratigraphical architecture at the muddy margin of the Cretaceous Western Interior Seaway, southern Utah: Sedimentology, v. 41, p. 521–542.

LEITHOLD, E.L., AND DEAN, W.E., 1998, Depositional processes and carbon burial on a Turonian prodelta at the margin of the Western Interior Seaway, in Dean, W.E., and Arthur, M.A., eds., Stratigraphy and Paleoenvironments of the Cretaceous Western Interior Seaway, U.S.A: SEPM, Concepts in Sedimentology and Paleontology, v. 6, p. 189–200.

LI, W., BHATTACHARYA, J.P., ZHU, Y., GARZA, D., AND BLANKENSHIP, E., 2011, Evaluating delta asymmetry using three-dimensional facies architecture and ichnological analysis, Ferron "Notom Delta," Capital Reef, Utah, USA: Sedimentology, v. 58, p. 478–507.

LI, Y., AND BHATTACHARYA, J.P., 2013, Facies-architecture study of a stepped, forced regressive compound incised valley in the Ferron Notom Delta, southern central Utah, U.S.A: Journal of Sedimentary Research, v. 83, p. 206–225.

LI, Y., AND SCHIEBER, J., 2015, On the origin of a phosphate enriched interval in the Chattanooga Shale (Upper Devonian) of Tennessee: a combined sedimentologic, petrographic, and geochemical study: Sedimentary Geology, v. 329, p. 40–61.

LI, Z., AND ASCHOFF, J., 2022a, Constraining the effects of dynamic topography on the development of Late Cretaceous Cordilleran foreland basin, western United States: Geological Society of America, Bulletin, v. 134, p. 446–462.

LI, Z., AND ASCHOFF, J., 2022b, Shoreline evolution in the Late Cretaceous North American Cordilleran foreland basin: an exemplar of the combined influence of tectonics, sea level, and sediment supply through time: Earth-Science Reviews, v. 226, no1. 03947.

LI, Z., BHATTACHARYA, J., AND SCHIEBER, J., 2015, Evaluating along-strike variation using thin-bedded facies analysis, Upper Cretaceous Ferron Notom Delta, Utah: Sedimentology, v. 62, p. 2060–2089.

LI, Z., AND SCHIEBER, J., 2018a, Detailed facies analysis of the Upper Cretaceous Tununk Shale Member, Henry Mountains Region, Utah: implications for mudstone depositional models in epicontinental seas: Sedimentary Geology, v. 364, p. 141–159.

LI, Z., AND SCHIEBER, J., 2018b, Composite particles in mudstones: examples from the Late Cretaceous Tununk Shale Member of the Mancos Shale Formation: Journal of Sedimentary Research, v. 88, p. 1319–1344.

LI, Z., AND SCHIEBER, J., 2020, Application of sequence stratigraphic concepts to the Upper Cretaceous Tununk Shale Member of the Mancos Shale Formation, south-central Utah: parasequence styles in shelfal mudstone strata: Sedimentology, v. 67, p. 118–151.

LIU, J.P., LI, A.C., XU, K.H., VELOZZI, D.M., YANG, Z.S., MILLIMAN, J.D., AND DEMASTER, D.J., 2006, Sedimentary features of the Yangtze River-derived along-shelf clinoform deposit in the East China Sea: Continental Shelf Research, v. 26, p. 2141–2156.

LOUTIT, T.S., HARDENBOL, J., VAIL, P.R., AND BAUM, G.R., 1988, Condensed sections: the key to age determination and correlation of continental margin sequences, in Wilgus, C.K., Hastings, B.S., Ross, C.A., Posamentier, H., Van Wagoner, J.C., and Kendall, C.G.St.C., eds., Sea-Level Changes: An Integrated Approach: SEPM, Special Publication 42, p. 183–216.

MACEACHERN, J.A., BANN, K.L., BHATTACHARYA, J.P., AND HOWELL, C.D., JR., 2005, Ichnology of deltas: organism responses to the dynamic interplay of rivers, waves, storms, and tides, in Giosan, L., and Bhattacharya, J.P., eds., River Deltas: Concepts, Models, and Examples: SEPM, Special Publication 83, p. 49–85.

MACQUAKER, J.H.S., AND TAYLOR, K.G., 1996, A sequence-stratigraphic interpretation of a mudstone-dominated succession: the Lower Jurassic Cleveland Ironstone Formation, UK: Geological Society of London, Journal, v. 153, p. 759–770.

MACQUAKER, J.H.S., TAYLOR, K.G., AND GAWTHORPE, R.L., 2007, High-resolution facies analyses of mudstones: implications for paleoenvironmental and sequence stratigraphic interpretations of offshore ancient mud-dominated successions: Journal of Sedimentary Research, v. 77, p. 324–339.

MACQUAKER, J.H.S., BENTLEY, S.J., AND BOHACS, K.M., 2010, Wave-enhanced sediment-gravity flows and mud dispersal across continental shelves: reappraising sediment transport processes operating in ancient mudstone successions: Geology, v. 38, p. 947–950.

MIALL, A.D., AND ARUSH, M., 2001, The Castlegate Sandstone of the Book Cliffs, Utah: sequence stratigraphy, paleogeography, and tectonic controls: Journal of Sedimentary Research, v. 71, p. 537–548.

MIALL, A.D., CATUNEANU, O., VAKARELOV, B.K., AND POST, R., 2008, The Western Interior Basin, in Miall, A.D., eds., Sedimentary Basins of the World: Elsevier, p. 329–362.

MILLER, K.G., SUGARMAN, P.J., BROWNING, J.V., KOMINZ, M.A., OLSSON, R.K., FEIGENSON, M.D., AND HERNÁNDEZ, J.C., 2004, Upper Cretaceous sequences and sea-level history, New Jersey Coastal Plain: Geological Society of America, Bulletin, v. 116, p. 368–393.

MILLER, K.G., MOUNTAIN, G.S., BROWNING, J.V., KATZ, M.E., MONTEVERDE, D., SUGARMAN, P.J., ANDO, H., BASSETTI, M.A., BJERRUM, D., HESSELBO, S., KARAKAYA, S., PROUST, J.-N., AND RABINEAU, M., 2013, Testing sequence stratigraphic models by drilling Miocene foresets on the New Jersey shallow shelf: Geosphere, v. 9, p. 1236–1256.

MITCHUM, R.M., VAIL, P.R., AND THOMPSON, S., III, 1977, Seismic stratigraphy and global changes of sea level, part 2: the depositional sequence as a basic unit for stratigraphic analysis, in Payton, C.E., eds., Seismic Stratigraphy: Applications to Hydrocarbon Exploration: American Association of Petroleum Geologists, Memoir 26, p. 53–62.

NEAL, J.E., ABREU, V., BOHACS, K.M., FELDMAN, H.R., AND PEDERSON, K.H., 2016, Accommodation succession (δA/δS) sequence stratigraphy: observational method, utility and insights into sequence boundary formation: Geological Society of London, Journal, v. 173, p. 803–816.

OGG, J.G., HINNOV, L.A., AND HUANG, C., 2012, Cretaceous, in Gradstein, F.M., Ogg, J.G., Schmitz, M.D., and Ogg, G.M., eds., The Geologic Time Scale: Elsevier, p. 793–853.

PATRUNO, S., AND HELLAND-HANSEN, W., 2018, Clinoforms and clinoform systems: review and dynamic classification scheme for shorelines, subaqueous deltas, shelf edges and continental margins: Earth-Science Reviews, v. 185, p. 202–233.

PATRUNO, S., HAMPSON, G.J., AND JACKSON, C.A.L., 2015, Quantitative characterisation of deltaic and subaqueous clinoforms: Earth-Science Reviews, v. 142, p. 79–119.

PATTISON, S.A.J., 2019, Using classic outcrops to revise sequence stratigraphic models: reevaluating the Campanian Desert Member (Blackhawk Formation) to lower Castlegate Sandstone interval, Book Cliffs, Utah and Colorado, USA: Geology, v. 41, p. 11–14.

PETERSON, F., RYDER, R.T., AND LAW, B.E., 1980, Stratigraphy, sedimentology, and regional relationships of the Cretaceous System in the Henry Mountains region, Utah, in Picard, M.D., ed., Henry Mountains Symposium: Utah Geological Association, Publication 8, p. 151–170.

PIRMEZ, C., PRATSON, L.F., AND STECKLER, M.S., 1998, Clinoform development by advection-diffusion of suspended sediment: modeling and comparison to natural systems: Journal of Geophysical Research, Solid Earth, v. 103, p. 24,141–24,157.

PLINT, A.G., 2014, Mud dispersal across a Cretaceous prodelta: storm-generated, wave-enhanced sediment gravity flows inferred from mudstone microtexture and microfacies: Sedimentology, v. 61, p. 609–647.

POSAMENTIER, H.W., AND VAIL, P.R., 1988, Eustatic controls on clastic deposition II: sequence and systems tract models, in Wilgus, C.K., Hastings, B.S., Ross, C.A., Posamentier, H., Van Wagoner, J.C., and Kendall, C.G.St.C., eds., Sea-Level Changes: An Integrated Approach: SEPM, Special Publication 42, p. 125–154.

POSAMENTIER, H.W., ALLEN, G.P., JAMES, D.P., AND TESSON, M., 1992, Forced regressions in a sequence stratigraphic framework: concepts, examples, and exploration significance: American Association of Petroleum Geologists, Bulletin, v. 76, p. 1687–1709.

PRIMM, J.W., JOHNSON, C.L., AND STEARNS, M., 2018, Basin-axial progradation of a sediment supply driven distributive fluvial system in the Late Cretaceous southern Utah foreland: Basin Research, v. 30, p. 249–278.

RAISWELL, R., 1988, Evidence for surface reaction-controlled growth of carbonate concretions in shales: Sedimentology, v. 35, p. 571–575.

RAISWELL, R., AND FISHER, Q.J., 2000, Mudrock-hosted carbonate concretions: a review of growth mechanisms and their influence on chemical and isotopic composition: Journal of the Geological Society, v. 157, p. 239–251.

RIDENTE, D., AND TRINCARDI, F., 2005, Pleistocene "muddy" forced-regression deposits on the Adriatic shelf: a comparison with prodelta deposits of the late Holocene highstand mud wedge: Marine Geology, v. 222–223, p. 213–233.

SCHIEBER, J., 1998, Sedimentary features indicating erosion, condensation, and hiatuses in the Chattanooga Shale of central Tennessee: relevance for sedimentary and stratigraphic evolution, in Schieber, J., Zimmerle, W., and Sethi, P.S., eds., Shales and Mudstones: E. Schweizerbart'sche Verlagsbuchhandlung, p. 187–215.

SCHIEBER, J., 2016, Mud re-distribution in epicontinental basins: exploring likely processes: Marine and Petroleum Geology, v. 71, p. 119–133.

SCHIEBER, J., SOUTHARD, J., AND THAISEN, K., 2007, Accretion of mudstone beds from migrating floccule ripples: Science, v. 318, p. 1760–1763.

SHANLEY, K.W., AND MCCABE, P.J., 1995, Sequence stratigraphy of Turonian–Santonian strata, Kaiparowits Plateau, southern Utah, USA: implications for regional correlation and foreland basin evolution, in Van Wagoner, J.C., and Bertram, G.T., eds., Sequence Stratigraphy of Foreland Basin Deposits, Outcrop and Subsurface: Examples from the Cretaceous of North America: American Association of Petroleum Geologists, Memoir 64, p. 103–136.

STRONG, N., AND PAOLA, C., 2008, Valleys that never were: time surfaces versus stratigraphic surfaces: Journal of Sedimentary Research, v. 78, p. 579–593.

SZWARC, T.S., JOHNSON, C.L., STRIGHT, L.E., AND MCFARLANE, C.M., 2015, Interactions between axial and transverse drainage systems in the Late Cretaceous Cordilleran foreland basin: evidence from detrital zircons in the Straight Cliffs Formation, southern Utah, USA: Geological Society of America, Bulletin, v. 127, p. 372–392.

TAYLOR, A.M., AND GOLDRING, R., 1993, Description and analysis of bioturbation and ichnofabric: Journal of the Geological Society of London, v. 150, p. 141–148.

TAYLOR, K.G., AND MACQUAKER, J.H.S., 2014, Diagenetic alterations in a silt- and clay-rich mudstone succession: an example from the Upper Cretaceous Mancos Shale of Utah, USA: Clay Minerals, v. 49, p. 213–227.

TRABUCHO-ALEXANDRE, J., 2015, More gaps than shale: erosion of mud and its effect on preserved geochemical and palaeobiological signals, in Smith, D.G., Bailey, R.J., Burgess, P.M., and Fraser, A.J., eds., Strata and Time: Probing the Gaps in Our Understanding: Geological Society of London, Special Publication 404, p. 251–270.

VAIL, P.R., 1987, Seismic stratigraphy interpretation using sequence stratigraphy, Part 1: seismic stratigraphy interpretation procedure, in Bally, A.W., eds., Atlas of Seismic Stratigraphy: American Association of Petroleum Geologists, Studies in Geology 27, p. 1–10.

VAN WAGONER, J.C., POSAMENTIER, H.W., MITCHUM, R.M., JR., VAIL, P.R., SARG, J.F., LOUTIT, T.S., AND HARDENBOL, J., 1988, An overview of the fundamentals of sequence stratigraphy and key definitions, in Wilgus, C.K., Hastings, B.S., Ross, C.A., Posamentier, H., Van Wagoner, J.C., and Kendall, C.G.S.C., eds., Sea-Level Changes: An Integrated Approach: SEPM, Special Publication 42, p. 39–45.

VAN WAGONER, J.C., VAN MITCHUM, R.M., CAMPION, K.M., AND RAHMANIAN, V.D., 1990, Siliciclastic Sequence Stratigraphy in Well Logs, Cores, and Outcrops: Concepts for High-Resolution Correlation of Time and Facies: American Association of Petroleum Geologists, Methods in Exploration Series, no. 7, 55 p.

WILSON, R.D., AND SCHIEBER, J., 2014, Muddy prodeltaic hyperpycnites in the lower Genesee Group of central New York, USA: implications for mud transport in epicontinental seas: Journal of Sedimentary Research, v. 84, p. 866–874.

ZELT, F.B., 1985, Natural gamma-ray spectrometry, lithofacies, and depositional environments of selected Upper Cretaceous marine mudrocks, western United States, including Tropic Shale and Tununk Member of Mancos Shale [Ph.D. Thesis]: Princeton University, 372 p.

ZHU, Y., BHATTACHARYA, J.P., LI, W., LAPEN, T.J., JICHA, B.R., AND SINGER, B.S., 2012, Milankovitch-scale sequence stratigraphy and stepped forced regressions of the Turonian Ferron Notom deltaic complex, south-central Utah, U.S.A: Journal of Sedimentary Research, v. 82, p. 723–746.